metals

MDPI

Article

Simplified Evaluation of Plastic Rotation Demand for Existing EBFs Equipped with Short Links

Rosario Montuori [1], Elide Nastri [2], Vincenzo Piluso [2] and Paolo Todisco [2,*]

[1] Department of Pharmacy, University of Salerno, 84084 Fisciano, SA, Italy; r.montuori@unisa.it
[2] Department of Civil Engineering, University of Salerno, 84084 Fisciano, SA, Italy; enastri@unisa.it (E.N.); v.piluso@unisa.it (V.P.)
* Correspondence: ptodisco@unisa.it

Abstract: The seismic events that occurred in the last decades have highlighted the importance of a correct design of the structures in seismic areas and the seismic inadequacy of a large part of the built heritage. Modern codes are still lacking in terms of prescriptions for the evaluation of the seismic performance of existing buildings. The present work proposes a simplified method for the evaluation of the demand in terms of plastic rotation for short links of steel Eccentrically Braced Frames (EBFs). A relationship for the evaluation of the demand, that exploits elastic analysis and rigid-plastic analysis extended to the second-order effects, is proposed. The calibration of this relationship was carried out on 420 EBFs equipped with short links designed according to three different approaches. The 420 frames have been also used to analyze the behavior in the plastic range of EBF type structures equipped with short links. The study also provides an extensive analysis on the influence of plastic redistribution capacity on the demand in terms of plastic rotations of links, corresponding to the achievement of the maximum bearing capacity. The obtained relation can be exploited as an assessment tool by comparing the demand with the link capacity. Moreover, from a performance-based design point of view, the same can be used for predicting the required ultimate plastic rotation as a function of the plastic redistribution capacity of the structure.

Keywords: pushovers; rigid-plastic analysis; capacity; demand; EBFs

Citation: Montuori, R.; Nastri, E.; Piluso, V.; Todisco, P. Simplified Evaluation of Plastic Rotation Demand for Existing EBFs Equipped with Short Links. *Metals* **2022**, *12*, 1002. https://doi.org/10.3390/met12061002

Academic Editor: Thomas Niendorf

Received: 7 May 2022
Accepted: 9 June 2022
Published: 10 June 2022

1. Introduction

The seismic events occurred in the last decades have highlighted the importance of a proper design of structures in seismic areas and the seismic inadequacy of a large part of the built heritage [1,2]. In particular, the social and media impact of the catastrophic consequences of these events, connected to the extreme vulnerability of the built heritage, has accompanied and pushed the introduction of modern standards on the design and verification of structures in seismic areas which, however, are still lacking in content in terms of evaluation of the seismic performance of existing buildings [3–8].

Much research has focused on the evaluation of the link overstrength considering the importance of this factor in the application of the hierarchy criteria [9–11], and some other experimental works have tried to lay the foundations for the empirical estimation of the ultimate plastic rotation of short, intermediate, and long links [12–20]. However, the ultimate rotation depends on several factors, such as the link length, the web slenderness, the spacing of stiffeners, and the steel grade [21,22].

The work herein presented aims to define a relationship for the evaluation of the demand in terms of plastic rotation for short links of steel Eccentrically Braced Frames (EBF). The plastic rotation is computed exploiting the concept of equivalent moment, which is the moment developing at the link ends due to the shear action. In fact, even though the short links are mainly interested by shear behavior, it is possible to compute, as suggested by codes [23–25], an equivalent plastic rotation γ_p (Figure 1).

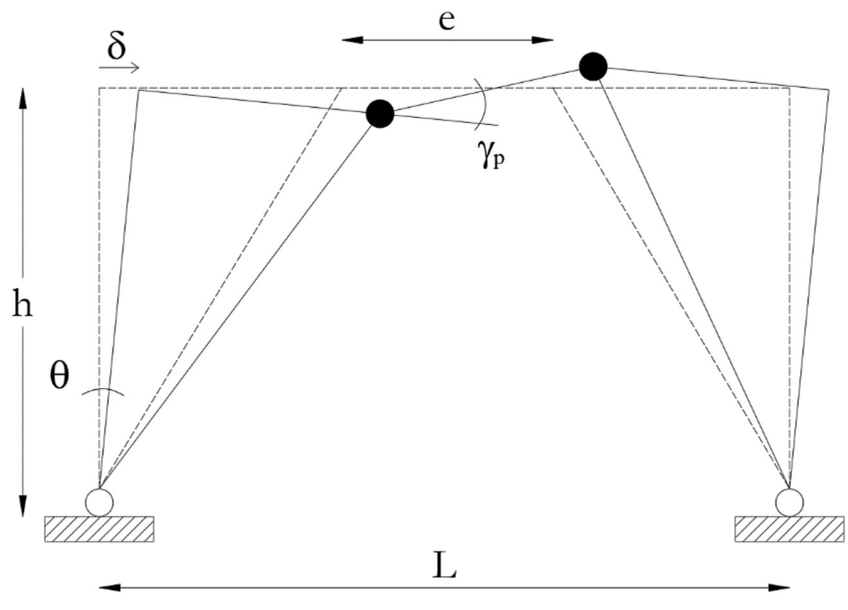

Figure 1. EBF scheme in deformed configuration.

The most important parameters governing the deformed configuration (Figure 1) are the top sway displacement δ, the rotation at the base of the columns θ, the equivalent plastic rotation γ_p , the eccentricity e, the bay span L, and the height h.

The demand refers to the achievement of the maximum bearing capacity of the structure [25–31].

The calibration of such relation is made using the result of the pushover analyses of 420 EBFs, with short links designed according to three different approaches [32–37].

The study is also accompanied by an extensive analysis on the influence of plastic redistribution capacity on the demand in terms of plastic rotations of the links, corresponding to the achievement of maximum bearing capacity of the structure.

2. Parametric Analysis

To define a simplified analytical methodology, it is necessary to rely on a large database of structures. To this scope, several Eccentrically Braced Frames (EBFs) were designed according to three approaches ranging from the most modern design philosophies, which aim to develop a global collapse mechanism, up to the oldest ones, which did not comply with specific requirements to be met in response to seismic actions [4–7].

The three design approaches are represented by three categories of frames [32,33]:

- Global Eccentrically Braced Frames (GEBFs)
- Special Eccentrically Braced Frames (SEBFs)
- Ordinary Eccentrically Braced Frames (ECBFs)

"Global" refers to structures designed with advanced methodologies capable of ensuring the development of global collapse mechanisms.

"Special", on the other hand, refers to structures designed through the application of the criteria provided by current European codes, in particular Eurocode 8 and which should avoid the development of "soft storey" mechanisms.

Finally, "Ordinary" refers to structures designed before modern anti-seismic codes, and which consequently do not comply with requirements aimed at dissipating incoming seismic energy. These structures, facing a seismic event, generally show collapse mechanisms essentially linked to the buckling of diagonals or columns.

For the parametric analysis, 140 geometric configurations were considered for which the parameters subject to variation were: the number of bays, n_b ranging from 2 to 6; the number of storeys, n_s ranging from 2 to 8; the bay span, equal to 3.00 m, 4.50 m, 6.00 m, 7.50 m. Considering the three different design approaches, the number of structures designed is 420. All combinations were analyzed considering permanent loads (G_k) equal to 3.5 kN/m^2, live loads (Q_k) equal to 3 kN/m^2, with an inter-storey height of 3.5 m. Steel grade is S275. The length of the seismic links has been fixed using the requirements of Eurocode 8 [23–25] which provides for short links ("I" and "H" shape cross-sections) [12–14]:

$$e \leq e_S = \alpha_S \cdot \frac{M_{p,link}}{V_{p,link}} \text{ with } \alpha_S = 1.6 \tag{1}$$

with

$$M_{p,link} = f_y \cdot b \cdot t_f \cdot \left(d - t_f\right) \tag{2}$$

$$V_{p,link} = \left(\frac{f_y}{\sqrt{3}}\right) \cdot t_w \cdot \left(d - t_f\right) \tag{3}$$

The symbology used is shown in Figure 2.

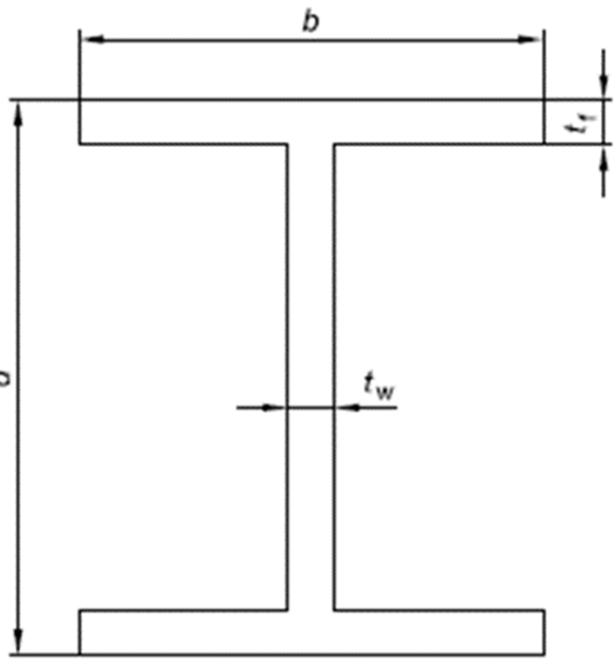

Figure 2. Symbology for link cross-section.

For short links, the Eurocode provides that the equivalent moment at the end of the links is calculated as follows:

$$M_{eq}^{short} = \frac{V_{p.link} \cdot e}{2} \tag{4}$$

where $V_{p.link}$ is reported in Equation (3) and e is the link length.

The designed EBFs have been subjected to pushover analyses, and for each structure the values of the plastic rotation of the first yielded element corresponding to development of the maximum bearing capacity were collected.

The push-over analyses are performed with SAP 2000 v21.0.2 software [38] in displacement control, considering both geometric and mechanical nonlinearities. The members are modelled as beam-column elements whose non-linearities are concentrated in plastic hinges at the element ends. Three types of plastic hinges have been modeled: Axial (P), Interacting P-M3, and Moment-M3. In Table 1, a summary with the characteristics of the plastic hinges, their location, and scope is reported [15–17]. The constitutive model of the plastic hinge is rigid perfectly plastic, and the plastic threshold is computed considering the nominal material properties. P-Hinge is applied according to the pattern reported in Figure 3.

Table 1. Summary diagram of plastic hinges on the SAP2000 model.

Type	Applied to:	Aim
Axial-P	Columns (centerline section) Bracing (centerline section)	Control the occurrence of mechanisms of axial instability of the element
Moment-M3	Links (end sections)	Control the plasticization of the dissipative element of the EBF structural type (Equivalent moment)
Interaction-P-M3	Columns (end sections)	Control the plasticization of the columns due to the interaction between normal stress and bending moment
colors refers to the hinge pattern showed in Figure 3		

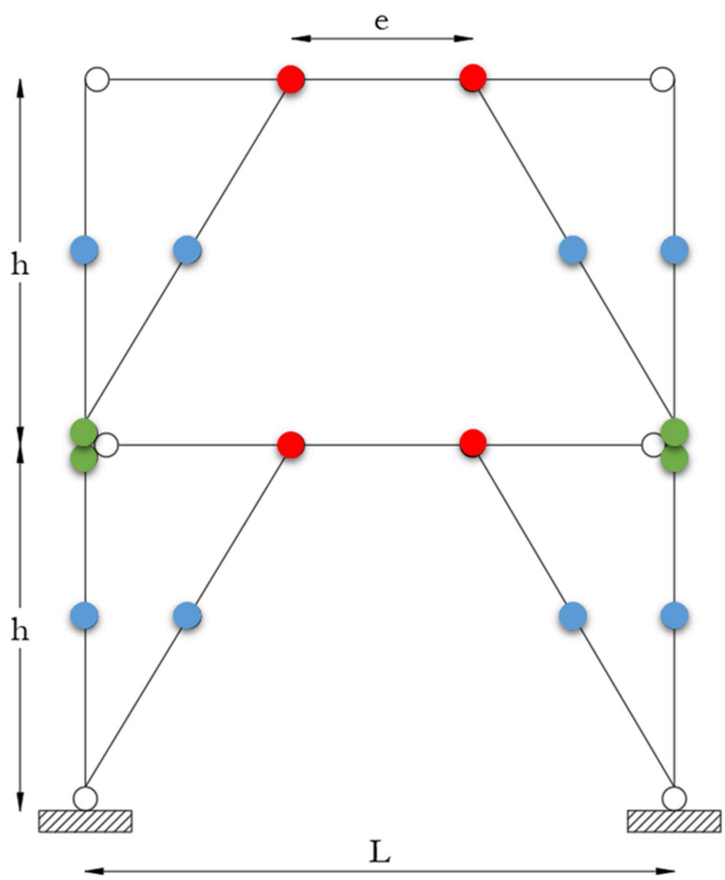

Figure 3. P-Hinge pattern.

3. Second-Order Rigid-Plastic Analysis for EBFs Equipped with Short Links

It is known that the maximum bearing capacity can be evaluated by the limit analysis and by exploiting the kinematic theorem of plastic collapse. Moreover, accounting for the second order effects, the kinematic theorem is extended to the concept of collapse mechanism equilibrium curve, which is a straight line (Equation (5)) [27,32,36,37] where α_0 is the first order collapse multiplier and γ_s is the slope of the collapse mechanism equilibrium curve:

$$\alpha = \alpha_0 - \gamma_s \delta \tag{5}$$

Given the sections of the columns, the links at each floor, and the static force distribution of an existing structure, it is easy to compute the first order collapse multipliers α_0 and, the slopes γ_s for each type of possible collapse mechanism. The mechanism that will be more prone to develop is the one corresponding to the curve characterized by the lower values of α (Equation (5)), in the range of displacements compatible with the local ductility resources, in this case, one of the links. For this reason, the collapse multiplier α_0 and the slope γ_s characterizing the analyzed frame will be those associated with the most likely mechanism. The possible collapse mechanisms are reported in Figure 4.

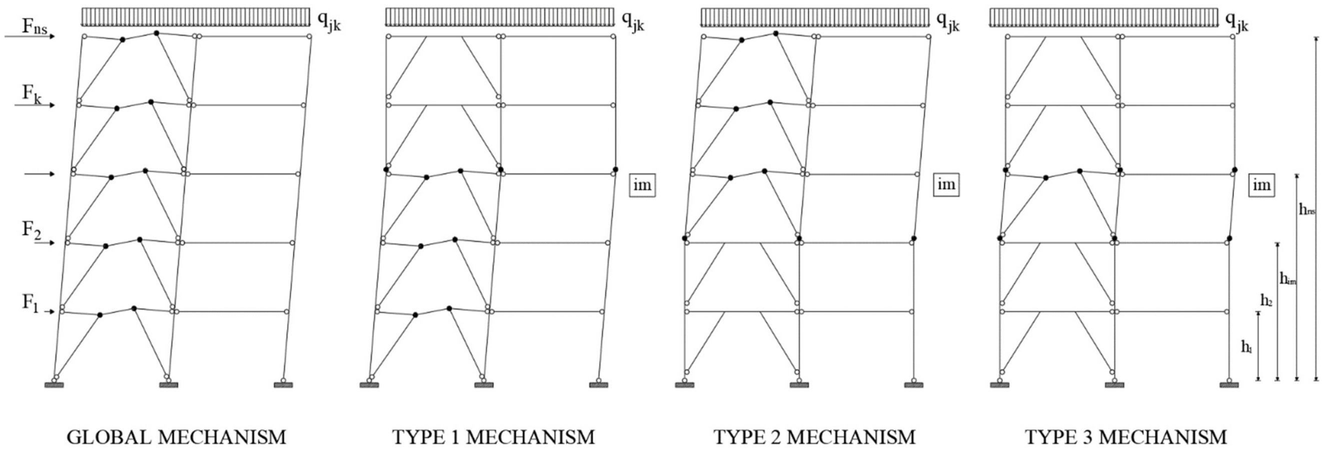

Figure 4. Collapse mechanism types for EBFs.

According to the theory of limit analysis, a rigid-plastic behavior of the structure is assumed until the complete development of the collapse mechanism. Consequently, the attention is focused on the condition in which the structure shows itself in the state of collapse, neglecting any intermediate condition [33,34].

For any given collapse mechanism, the mechanism equilibrium curve can be easily derived by equating the external work, due to seismic actions (first-order effects) to the internal work due to the plastic hinges involved in the collapse mechanism, provided that the second-order external work due to vertical loads is also evaluated. The internal and external work is calculated for a unit virtual rotation θ at the base of the columns (Figure 1). The relationships for the evaluation of the first order collapse multipliers for each possible collapse mechanism are reported [36,37]:

- for global collapse mechanism:

$$\alpha_0^{(g)} = \frac{\sum_{k=1}^{n_s} \sum_{j=1}^{n_s} W_{d,kj}}{\sum_{k=1}^{n_s} F_k \cdot h_k} \tag{6}$$

- for type-1 mechanism:

$$\alpha_{0,i_m}^{(1)} = \frac{\sum_{i=1}^{n_c} M_{ci,i_m+1} + \sum_{k=1}^{i_m} \sum_{j=1}^{n_b} W_{d,kj}}{\sum_{k=1}^{i_m} F_k \cdot h_k + h_{i_m} \cdot \sum_{k=i_m+1}^{n_s} F_k} \tag{7}$$

- for type-2 mechanism:

$$\alpha_{0,i_m}^{(2)} = \frac{\sum_{i=1}^{n_c} M_{ci,i_m} + \sum_{k=i_m}^{n_s} \sum_{j=1}^{n_b} W_{d,kj}}{\sum_{k=i_m}^{n_s} F_k \cdot (h_k + h_{i_m-1})} \tag{8}$$

- for type-3 mechanism:

$$\alpha_{0,i_m}^{(3)} = \frac{\sum_{i=1}^{n_c} M_{ci,i_m+1} + \sum_{j=1}^{n_b} W_{d,i_mj}}{(h_{i_m} + h_{i_m-1}) \cdot \sum_{k=i_m}^{n_s} F_k} \ ; i_m = 1 \tag{9}$$

$$\alpha^{(3)}_{0,i_m} = \frac{\sum_{i=1}^{n_c} M_{ci,i_m} + \sum_{i=1}^{n_c} M_{ci,i_m+1} + \sum_{j=1}^{n_b} W_{d,i_m j}}{(h_{i_m} + h_{i_m-1}) \cdot \sum_{k=i_m}^{n_s} F_k}\ ; i_m = 2, 3, \ldots, n_s \tag{10}$$

where the internal work of dissipative zones, for a unit rotation at the base of the columns, is given by:

$$W_{d.kj} = 2M^{short}_{eq,kj} \cdot \frac{L_{kj}}{e_{kj}} \tag{11}$$

where $M^{short}_{eq,kj}$ is the equivalent moment of short links [18–20], L_{kj} is the length of the bay hosting the link at the k-th storey, and e_{kj} is the length of the link at the k-th storey. Considering the relationship between the rotation of the ends of the links and that at the base of the columns (Figure 1), the link rotation can be expressed as follows:

$$\gamma_{link} = \theta_{bc} \cdot \frac{L_{kj}}{e_{kj}} \tag{12}$$

It is observed that in Equations (6)–(11), k, j and i are respectively the storey, the bay, and the column index. The seismic design horizontal actions for each storey are defined as F_k, while h_k and h_{i_m} are, respectively, the height of the k-th storey and the height of the i_m-th storey, where i_m is the mechanism index. n_b, n_c, and n_s are respectively the number of bays (index j), columns (index i), and storeys (index k).

As regards the slopes of the mechanism equilibrium curve, for each type of mechanism, they are defined as follows:

- for global collapse mechanism:

$$\gamma^{(g)} = \frac{1}{h_{n_s}} \frac{\sum_{k=1}^{n_s} V_k h_k}{\sum_{k=1}^{n_s} F_k h_k} \tag{13}$$

- for type-1 mechanism:

$$\gamma^{(1)}_{i_m} = \frac{1}{h_{i_m}} \frac{\sum_{k=1}^{i_m} V_k h_k + h_{i_m} \sum_{k=i_m+1}^{n_s} V_k}{\sum_{k=1}^{i_m} F_k h_k + h_{i_m} \sum_{k=i_m+1}^{n_s} F_k} \tag{14}$$

- for type-2 mechanism:

$$\gamma^{(2)}_{i_m} = \frac{1}{h_{n_s} - h_{i_m-1}} \frac{\sum_{k=i_m}^{n_s} V_k (h_k - h_{i_m-1})}{\sum_{k=i_m}^{n_s} F_k (h_k - h_{i_m-1})} \tag{15}$$

- for type-3 mechanism:

$$\gamma^{(3)}_{i_m} = \frac{1}{h_{i_m} - h_{i_m-1}} \frac{\sum_{k=i_m}^{n_s} V_k}{\sum_{k=i_m}^{n_s} F_k} \tag{16}$$

where V_k is the total vertical load acting on the k-th storey.

4. Evaluation of the Maximum Multiplier through Second-Order Rigid-Plastic Analysis

The analytical formulation proposed to define the multiplier α_{max} corresponding to the achievement of the maximum bearing capacity has its bases in the Merchant–Rankine formula [32–40]. This relationship allows the determination of α_{max} as a combination between the collapse multiplier obtained from a first-order rigid-plastic analysis α_0 and the elastic critical multiplier of gravitational loads α_{cr}:

$$\frac{1}{\alpha_{max}} = \frac{1}{\alpha_0} + \frac{1}{\alpha_{cr}} \tag{17}$$

and considering that $1/\alpha_{cr} \approx \gamma = \gamma_s \delta_1$, [39,40] Equation (17) can be rearranged as:

$$\alpha_{max} = \frac{\alpha_0}{1 + \Psi_{EBF}\alpha_0\gamma_s\delta_1} \tag{18}$$

Ψ_{EBF} is a corrective coefficient, function of the ratio between the extensional stiffness of the bracings and the flexural stiffness of the columns and the ratio between the flexural stiffness of the links and the flexural stiffness of the columns. All the properties are referred to members of the first storey.

$$\Psi_{EBF} = \overline{a} + \overline{b}\xi_1 + \overline{c}\xi_2 \tag{19}$$

$$\xi_1 = \frac{\sum_{i=1}^{n_{bc}} \frac{EA_{diag,i1}}{L_{diag,i1}} \cos^2\psi_{i1}}{\sum_{i=1}^{n_{cc}} \frac{EI_{c,i1}}{h^3_{c,i1}}} \tag{20}$$

$$\xi_2 = \frac{\sum_{j=1}^{n_{bc}} \frac{EI_{link,j1}}{e_{link,j1}}}{\sum_{i=1}^{n_{cc}} \frac{EI_{c,i1}}{h_{c,i1}} + \sum_{i=1}^{n_{c,nc}} \frac{EI_{c,i1}}{h_{c,i1}}} \tag{21}$$

$$\psi_{i1} = \tan^{-1}\left[\frac{h_{c,i1}}{\frac{1}{2}\left(L_{b,j1} - e_{link,j1}\right)}\right] \tag{22}$$

where $A_{diag,i1}$ is the area of the cross-section of the i-th diagonal at the first storey of the single frame; $L_{diag,i1}$ is the length of the i-th diagonal at the first storey of the single frame; ψ_{i1} is the inclination of the i-th diagonal at the first storey frame with respect to the horizontal direction; $h_{c,i1}$ is the height of the i-th column at the first storey belonging only to the braced bays of the single frame; $L_{b,j1}$ is the length of the braced j-th bay at the first storey; $e_{link,j1}$ is the length of the link of the j-th bay at the first storey; $I_{c,i1}$ is the moment of inertia along the strong axis of the i-th column at the first storey belonging only to the braced spans of the single frame; $I_{link,j1}$ is the moment of inertia along the strong axis of the link of the j-th span at the first storey; E is the Young modulus.

To calibrate the corrective coefficient Ψ, several numerical analyses were carried out to determine a, b, and c with the aim of minimizing the differences between the values obtained analytically and those obtained from non-linear static analyses, considering SEBFs and GEBFs. The OEBFs were excluded from the parametric analysis as they do not have any plastic redistribution capacity of stresses as the collapse is governed by phenomena of local instability of the diagonals and/or columns. In Table 2, the values obtained for the regression coefficients are reported.

Table 2. Regression coefficients ($\alpha_{\max}$).

	$\overline{a}$	$\overline{b}$	$\overline{c}$
SEBFs + GEBFs	2.4636	3.6962×10^{-5}	0.9873
SEBFs	−0.2514	0.0126	3.0734
GEBFs	6.8450	−0.00136	0.0127

In Figures 5–7 the results of the regression analysis are reported.

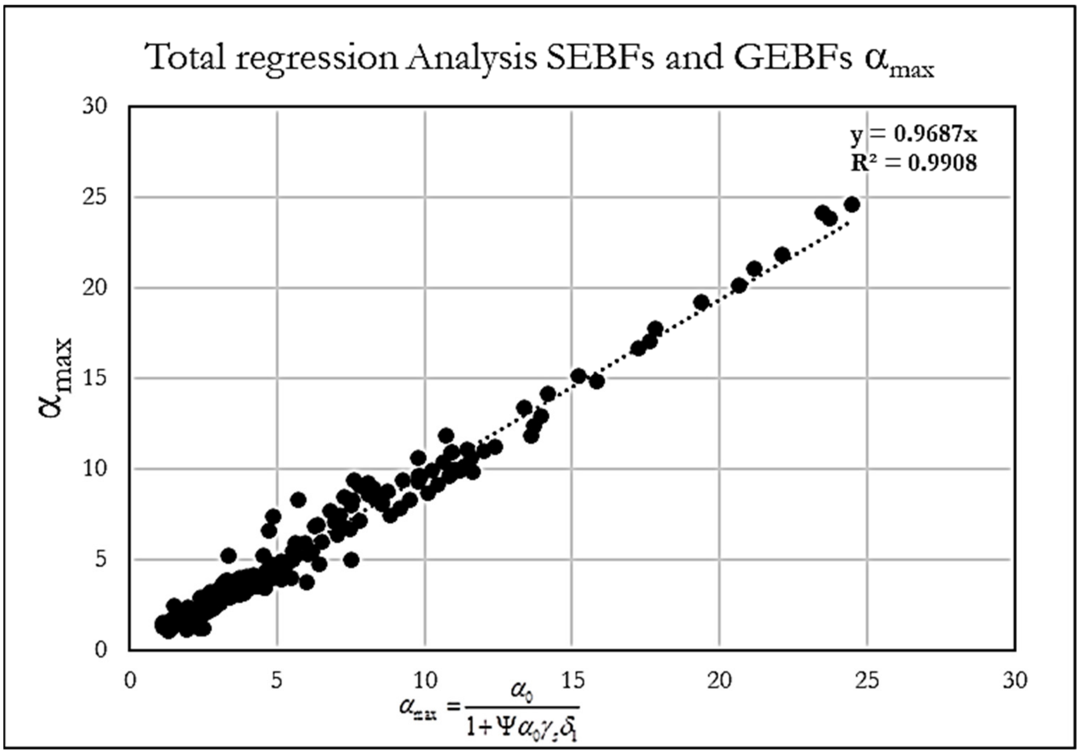

Figure 5. Regression analysis for the evaluation of α_{max} for SEBFs and GEBFs.

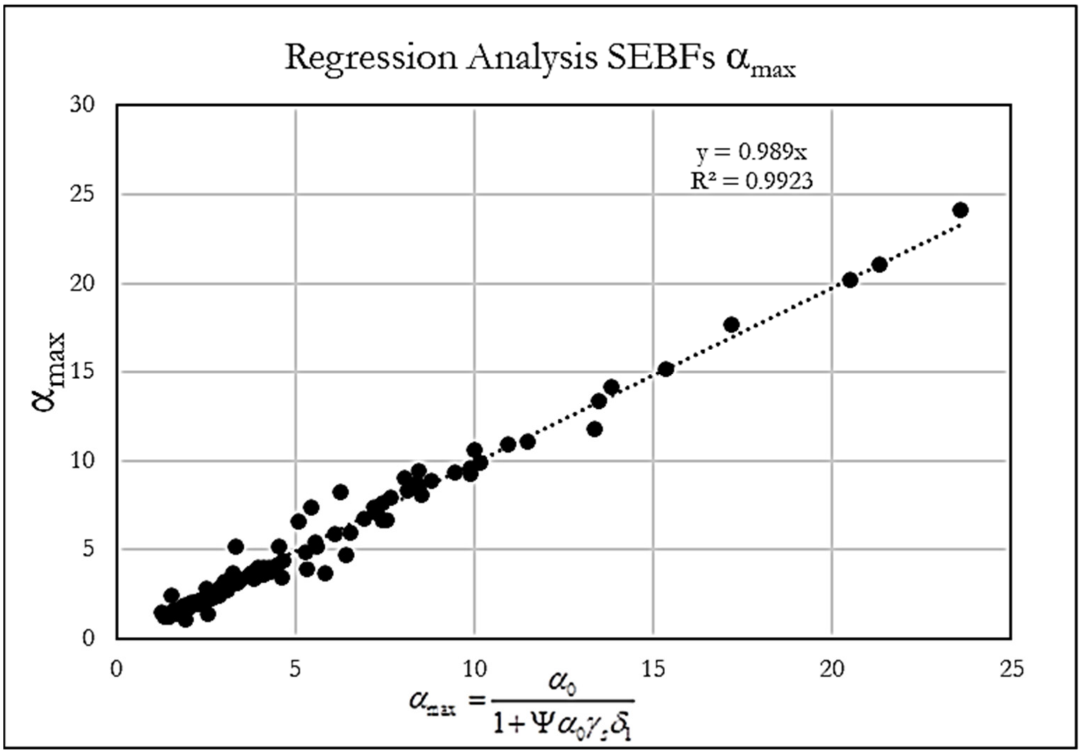

Figure 6. Regression analysis for the evaluation of α_{max} for SEBFs.

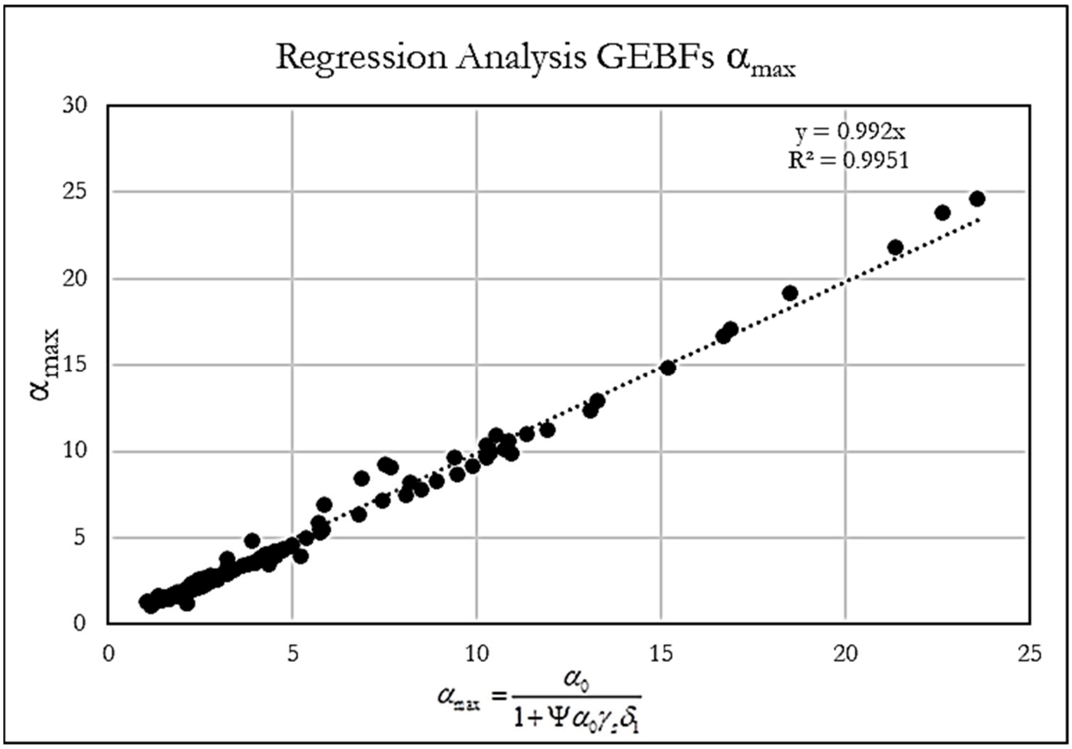

Figure 7. Regression analysis for the evaluation of α_{max} for SEBFs and GEBFs.

5. Simplified Evaluation of the Plastic Rotation Demand Corresponding to the Maximum Multiplier of Horizontal Forces

The prediction of the behavior of EBFs passes through the evaluation of the demand in terms of plastic rotations of the ends of the links, upon reaching the maximum bearing capacity. An analytical formulation based on a simplified model is proposed. It is considered a single-storey EBF (Figure 8), equipped with plastic redistribution capacity (typical of multi-storey and multi-span structures). For this purpose, two lateral stiffness values have been defined. A first value K_1 is valid until the elastic threshold is reached, and K_2 post-yielding stiffness, valid until the formation of the collapse mechanism occurs.

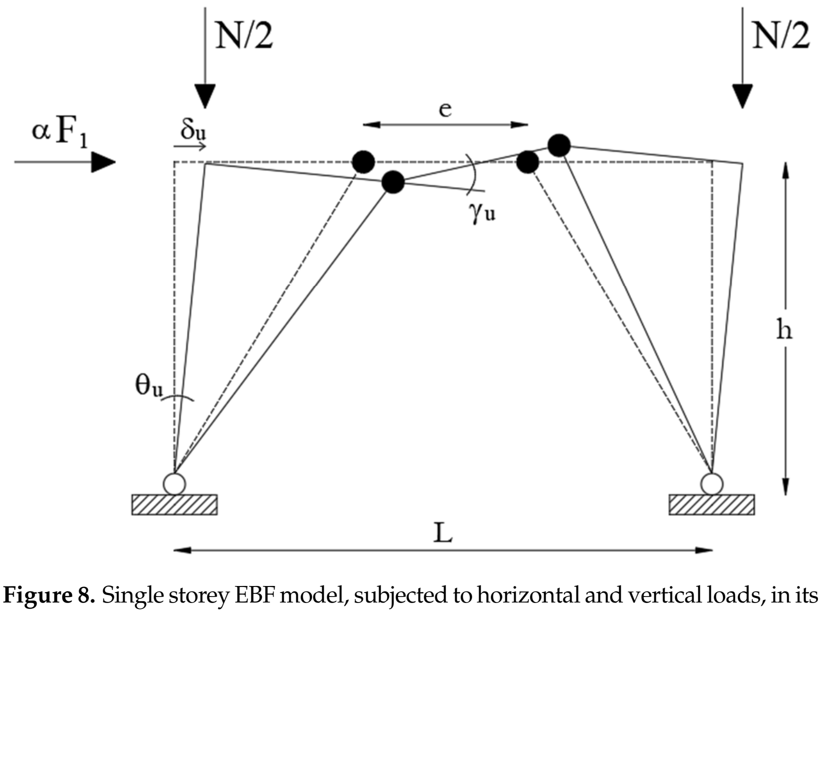

Figure 8. Single storey EBF model, subjected to horizontal and vertical loads, in its collapse configuration.

The frame is subjected to the vertical load N, and to the horizontal force F. At the elastic threshold, considering the second-order effects, the equilibrium in the horizontal direction provides (first yielding condition) [39,40]:

$$\alpha_y F_1 + \frac{N\delta_y}{h} = K_1 \delta_y \tag{23}$$

At the activation of the collapse mechanism, the plastic top-sway displacement δ_{Pl} is given by:

$$\delta_{Pl} = \delta_{mec} - \delta_y \tag{24}$$

where δ_{mec} is the top-sway displacement corresponding to the formation of the plastic mechanism.

As a result of the first yielding, there is also a reduction in the lateral stiffness of the frame, so that in the plastic field the lateral stiffness will be $K_2 < K_1$ (Figure 9).

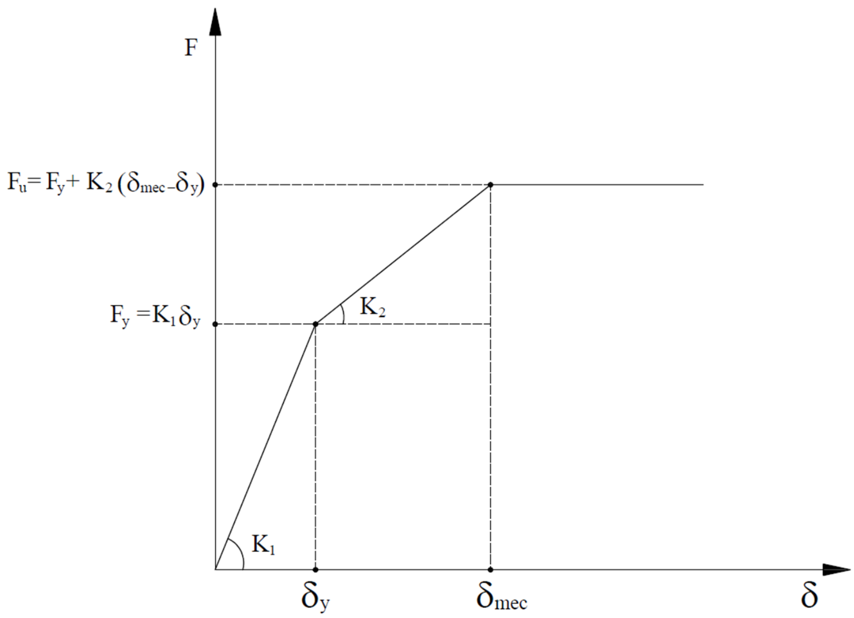

Figure 9. Lateral stiffness model adopted for the analysed structural scheme.

In collapse condition, the horizontal direction equilibrium changes and becomes:

$$\alpha_y F_1 + \frac{N\delta_y}{h} = K_1 \delta_y + K_2 \left(\delta_{mec} - \delta_y\right) \tag{25}$$

Obtaining δ_y from the Equation (23):

$$\delta_y = \frac{1}{K_1}\left(\alpha_y F_1 + \frac{N\delta_y}{h}\right) \tag{26}$$

That replaced in the Equation (25) gives:

$$\alpha_y F_1 + \frac{N\delta_y}{h} = K_1 \frac{1}{K_1}\left(\alpha_y F_1 + \frac{N\delta_y}{h}\right) + K_2 \left(\delta_{mec} - \delta_y\right) \tag{27}$$

Rearranging Equation (27) appropriately, returns:

$$\left(\delta_{mec} - \delta_y\right) = \frac{1}{K_2}\left[\left(\alpha_u - \alpha_y\right)F_1 + \frac{N}{h}\left(\delta_{mec} - \delta_y\right)\right] \tag{28}$$

Returning to the first yielding condition (23), it is possible to obtain F_1 as follows:

$$F_1 = \frac{K_1}{\alpha_y}\delta_y\left(1 - \frac{N}{K_1 h}\right) \tag{29}$$

Provided that:

$$\gamma = \frac{N}{K_1 h} \tag{30}$$

Equation (29) becomes:

$$F_1 = \frac{K_1}{\alpha_y}\delta_y(1-\gamma) \tag{31}$$

Substituting the Equation (31) in the Equation (28), it is obtained:

$$\left(\delta_{mec} - \delta_y\right) = \frac{1}{K_2}\left[\left(\alpha_u - \alpha_y\right)\frac{K_1}{\alpha_y}\delta_y(1-\gamma) + \frac{N}{h}\left(\delta_{mec} - \delta_y\right)\right] \tag{32}$$

Factoring out $\left(\delta_{mec} - \delta_y\right)$ and multiplying and dividing by K_1 you get:

$$\left(\delta_{mec} - \delta_y\right)\left(1 - \frac{K_1}{K_2}\frac{N}{K_1 h}\right) = \frac{K_1}{K_2}\left[\frac{\left(\alpha_u - \alpha_y\right)}{\alpha_y}\delta_y(1-\gamma)\right] \tag{33}$$

from which, recalling the Equations (30) and (24), it is obtained:

$$\frac{\delta_{Pl}}{\delta_y} = \frac{K_1}{K_2}\left(\frac{\alpha_u}{\alpha_y} - 1\right)\frac{(1-\gamma)}{\left(1 - \frac{K_1}{K_2}\gamma\right)} \tag{34}$$

The plastic rotations at the base of the structure θ_{Pl} are directly related to displacement δ_{Pl} through the height h considering a rigid collapse mechanism. As a result, the (34) can be written as:

$$\theta_{Pl} = c\frac{K_1}{K_2}\left(\frac{\alpha_u}{\alpha_y} - 1\right)\frac{\delta_y}{h}\frac{(1-\gamma)}{\left(1 - \frac{K_1}{K_2}\gamma\right)} \tag{35}$$

where c is a corrective coefficient linked to the structural typology and to the conversion from displacements to rotations.

Having to adapt the Equation (35) to multi-storey structures, it is better to express h as H_0/n_s where H_0 is the mechanism height of the examined structure and n_s is the number of storeys of the structure.

Having to express the relationship in terms of rotation of the links ends, it is necessary to convert the rotation θ_{Pl} for columns, in the rotation γ_{Pl} of the ends of the link, thus obtaining:

$$\frac{\gamma_{Pl}}{\delta_y}\frac{H_0}{n_s} = c\frac{K_1}{K_2}\left(\frac{\alpha_u}{\alpha_y} - 1\right)\frac{(1-\gamma)}{\left(1 - \frac{K_1}{K_2}\gamma\right)}\frac{L_b}{e} \tag{36}$$

Similarly, the relationship to evaluate the plastic rotations corresponding to the achievement of the maximum bearing capacity is given in the form:

$$\gamma_{p.\alpha_{max}} = \frac{\Psi_1}{\Psi_2}\Psi_3\left(\frac{\alpha_{max}}{\alpha_y} - 1\right)^{\Psi_4}\frac{1 - \Psi_5\gamma_s}{1 - \Psi_6\gamma_s}\frac{L}{e}\frac{n_s\delta_y}{H_0} \tag{37}$$

where α_y is the multiplier of horizontal forces corresponding to the formation of the first plastic hinge.

The Ψ_i coefficients, introduced in (37), have been determined by regression analysis and are given in the following form:

$$\Psi_1 = a_1 + b_1 n_b \tag{38}$$

$$\Psi_2 = a_2 + b_2 n_s \tag{39}$$

$$\Psi_3 = a_3 + c_3 \xi_2 \tag{40}$$

$$\Psi_4 = a_4 + c_4 \xi_2 \tag{41}$$

$$\Psi_5 = a_5 + c_5 \xi_2 \tag{42}$$

$$\Psi_6 = a_6 + c_6 \xi_2 \tag{43}$$

where n_b is the number of bays and ξ_2 is provided by the Equation (21).

The regression analysis was conducted separately for SEBFs and GEBFs, but in both cases a coefficient of determination R^2 close to the unit has been obtained.

The calibrated parameters are shown in Table 3.

Table 3. Regression coefficients ($\gamma_{p,\alpha\max}$).

Parameter	SEBFs	GEBFs
a_1	0.54227	2.624266
a_2	0.01232	4.272265
a_3	0.004938	0.404644
a_4	0.313962	0.533073
a_5	0.497981	1.371725
a_6	0.508882	1.504369
b_1	0.03707	−0.36372
b_2	−0.0014	−0.42819
c_3	−0.00569	−0.45676
c_4	−0.0925	0.028701
c_5	−0.22014	1.400378
c_6	−0.20562	0.849522

The results are reported in Figures 10 and 11 where on the x axis is reported as the plastic rotation obtained through the analytical formulation, while on the y the plastic rotation obtained by the pushovers is reported. To minimize the differences between the analytic formulation and the pushover values, the trendline has to show a slope close to the bisector, the regression points have to lean against the trend line and the determination coefficient R^2 has to be close to the unit. All these characteristics are respected with a good degree of precision in Figures 10 and 11.

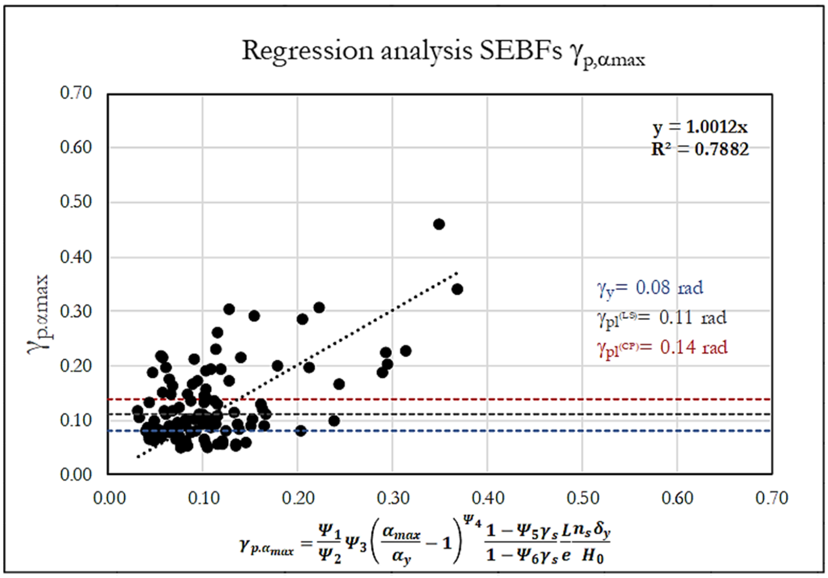

Figure 10. Regression analysis for the evaluation of $\gamma_{\alpha_{max}}$ for SEBFs.

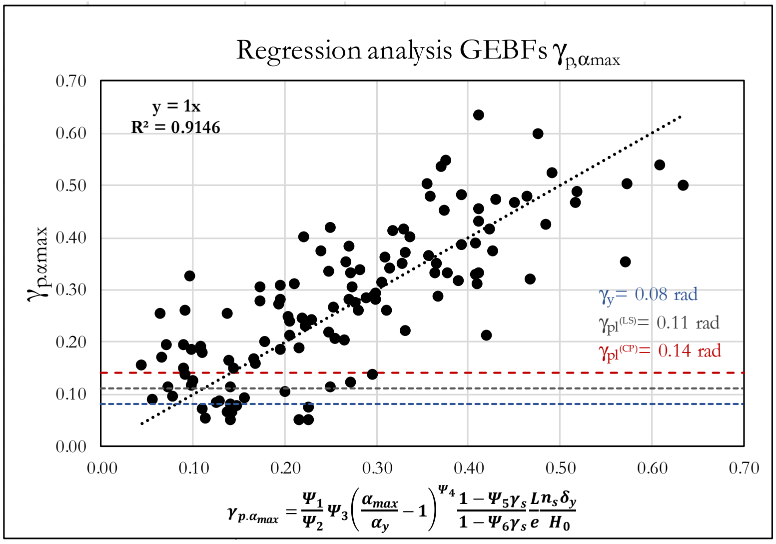

Figure 11. Regression analysis for the evaluation of $\gamma_{\alpha_{max}}$ for GEBFs.

6. Analysis of the Plastic Rotation Demand and Plastic Redistribution Capacity

The evaluation of the plastic rotation demand and the plastic redistribution capacity plays an important role in the evaluation of the behavior of EBFs. From the analysis of Figures 10 and 11, it is possible to draw some considerations regarding the demand in terms of plastic rotation corresponding to the achievement of the maximum bearing capacity [40,41]. The rotational capacity limits have been set in accordance with Eurocode 8 and FEMA 356 (USA), as reported in Table 4.

Table 4. Rotation capacity limits for short links (γ_{pl}).

γ_y **= 0.08 rad**	**Is the Elastic Limit Rotation of Short Links as Suggested by EC8;**
$\gamma_{Pl}^{(LS)} = 0.11$ rad	is the plastic rotation of short links for primary effects at the Life Safety (LS) performance level as established by FEMA 356 (USA)
$\gamma_{Pl}^{(CP)} = 0.14$ rad	is the plastic rotation of short links for primary effects at the Collapse Prevention (CP) performance level as established by FEMA 356 (USA)

It can be observed that:

- SEBFs equipped with short links exceed the rotational limit imposed for Collapse prevention (CP) by 30%, the limit imposed for Life Safety (LS) by 40%, and the limit imposed for the elastic threshold by 70%.
- GEBFs equipped with short links exceed the rotational limit imposed for Collapse prevention (CP) by 65%, the limit imposed for Life Safety (LS) by 70%, and the limit imposed for the elastic threshold by 75%.

SEBFs are frames that have shown from rigid-plastic analysis partial collapse mechanisms and lower collapse multipliers. It is unlikely that GEBFs showed global collapse mechanisms and higher collapse multipliers. Considering this, the GEBFs showed the need for greater excursion (rotation demand) in plastic field, together with the achievement of larger top sway displacements, to develop the maximum bearing capacity.

A fundamental parameter for the analysis of behavior in the plastic phase is the ratio α_{max}/α_y, representative of the plastic redistribution capacity of the analyzed structure. An extensive study on the link between the parameter α_{max}/α_y and the demand for plastic rotations $\gamma_{p.\alpha_{max}}$ has been carried out, grouping the structures for different parameters, to assess the field of application of the proposed formulation. For SEBFs in Figures 12–14, the results for the groups n_b (number of bays), n_s (number of storeys), and L_b (bay span) are reported.

SEBFs—nb

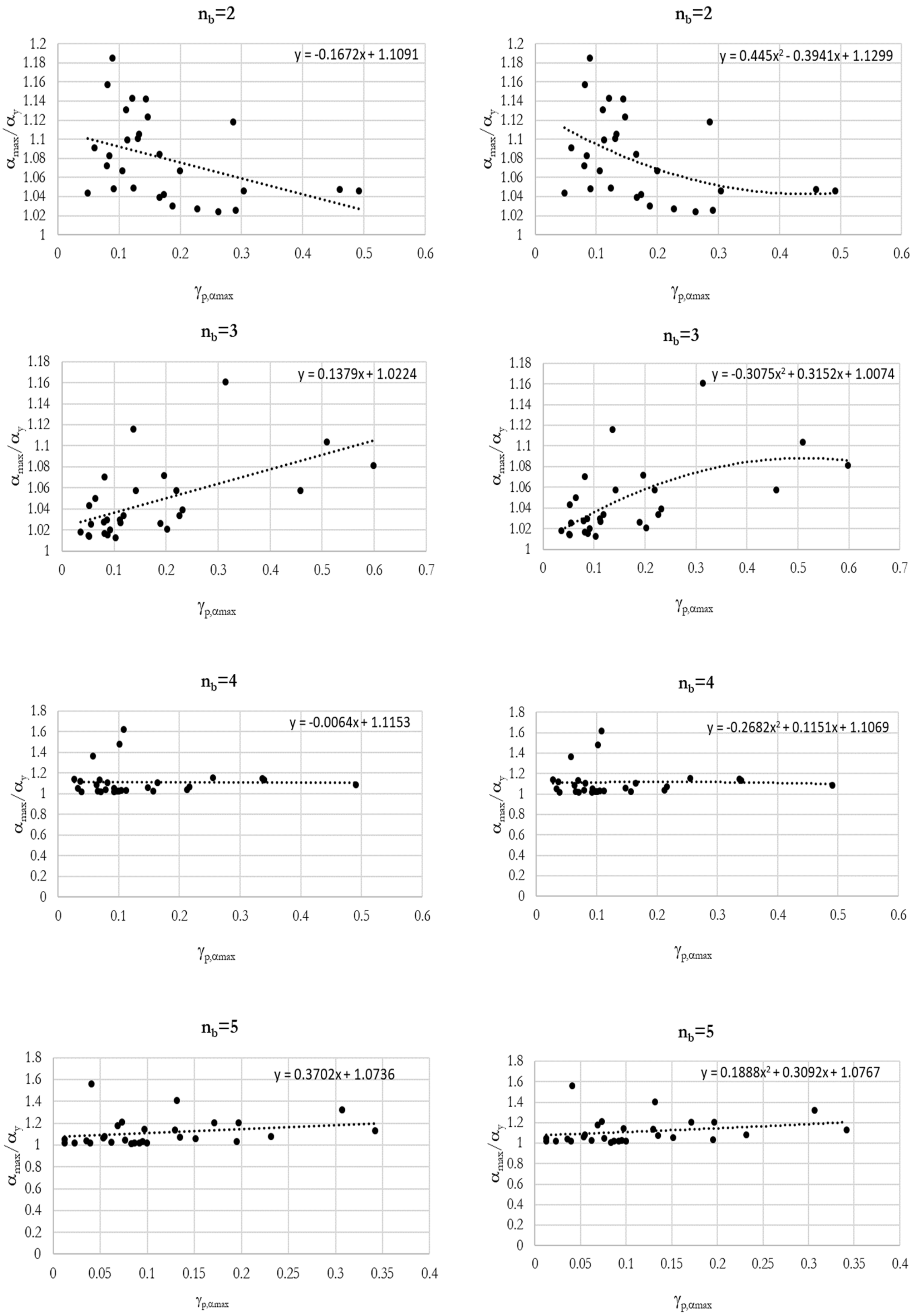

Figure 12. *Cont*.

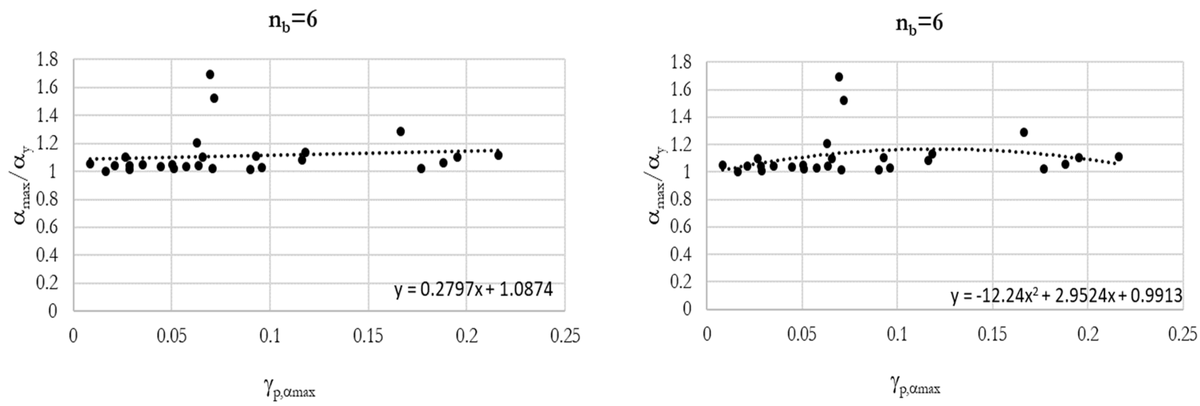

Figure 12. $\alpha_{max}/\alpha_y - \gamma_{p.\alpha_{max}}$ diagram for SEBFs: group for number of bays.

SEBFs—n$_s$

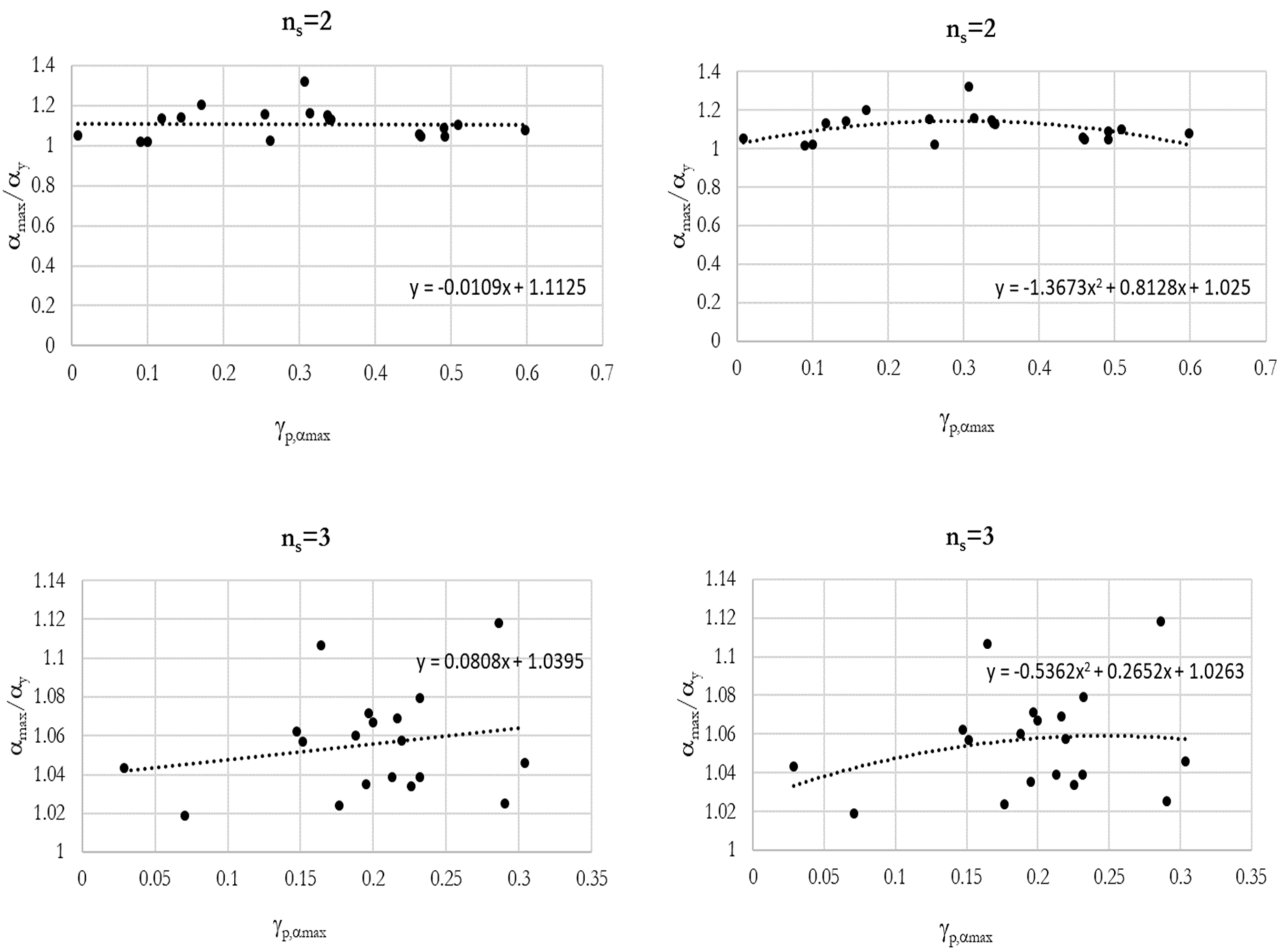

Figure 13. *Cont.*

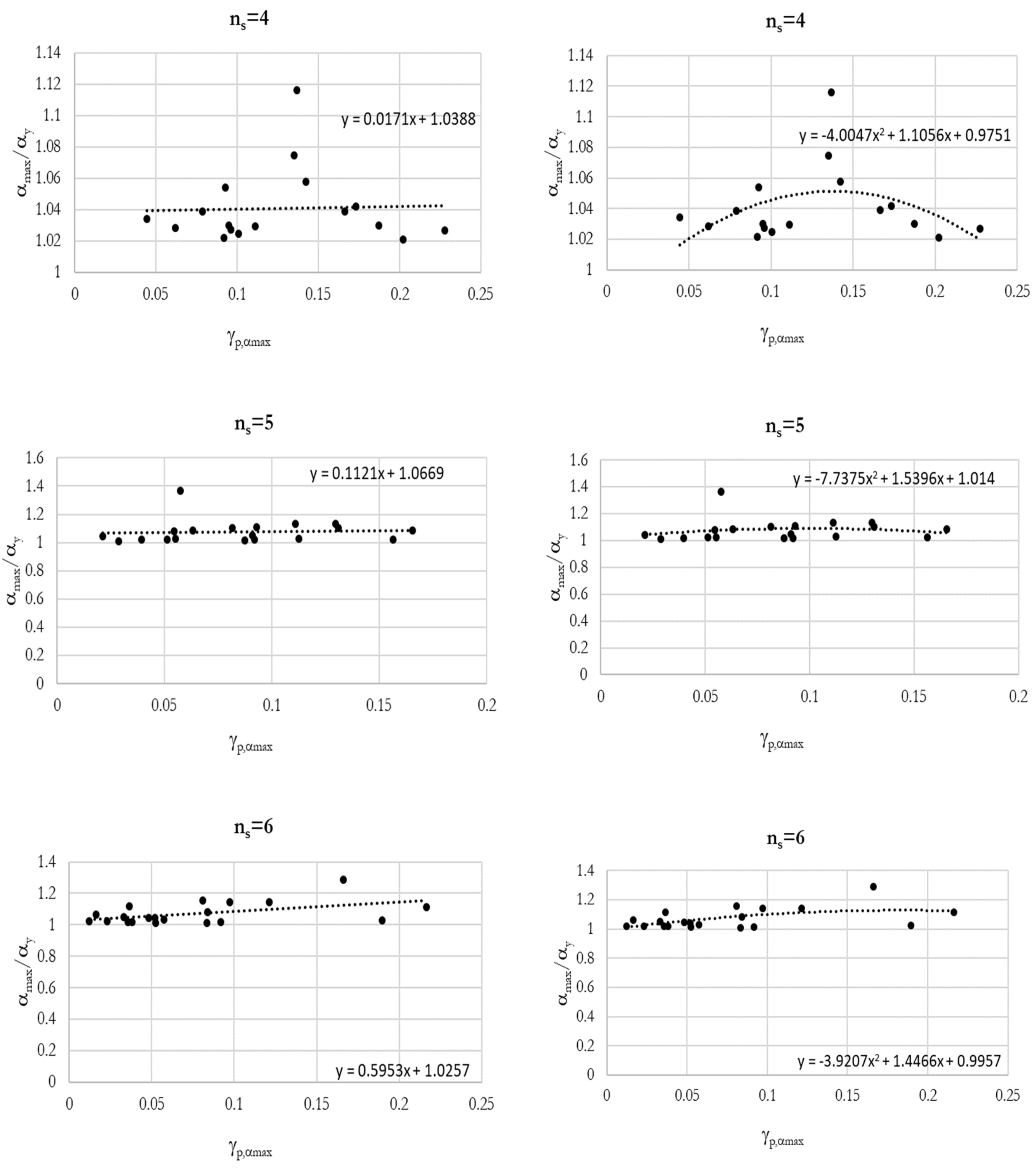

Figure 13. *Cont*.

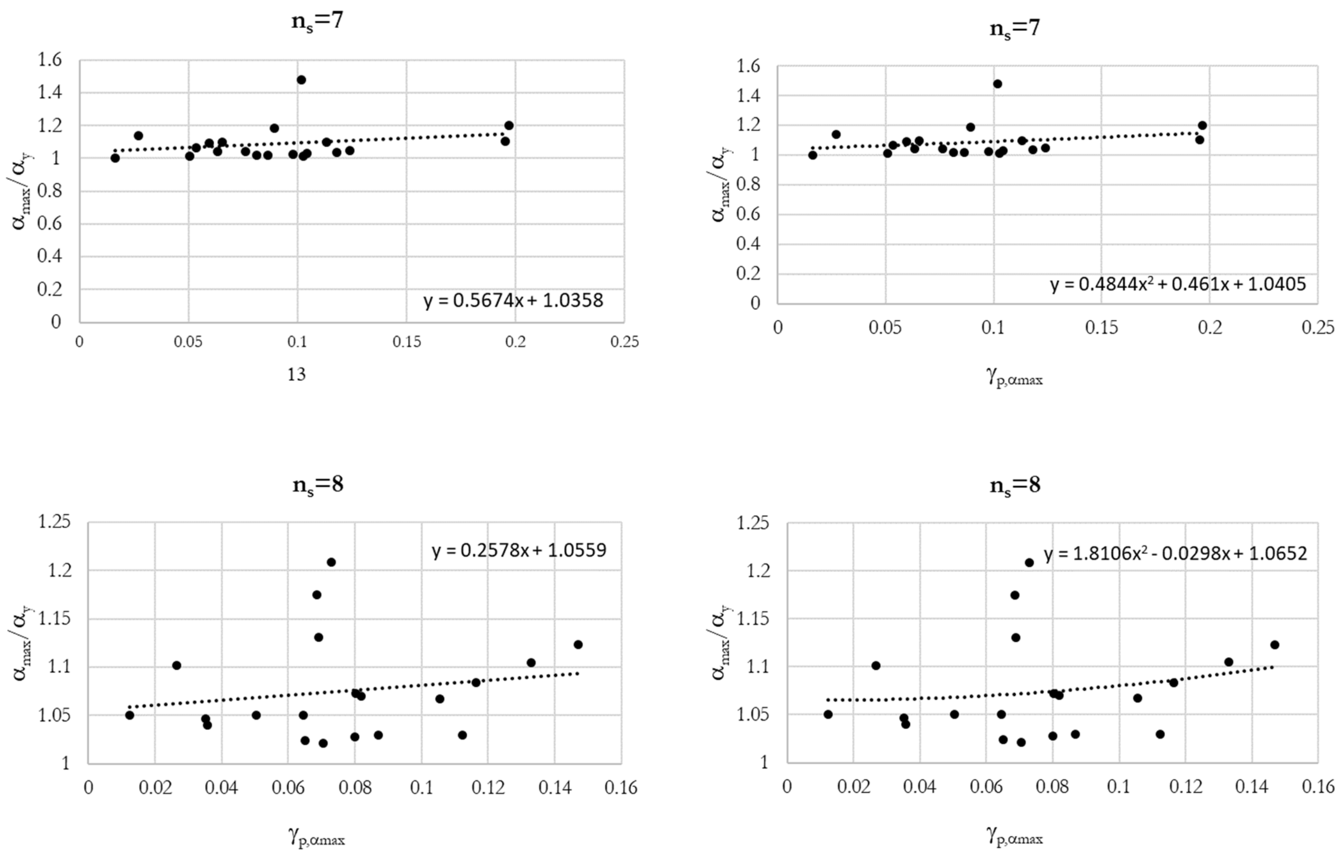

Figure 13. $\alpha_{max}/\alpha_y - \gamma_{p.\alpha_{max}}$ diagram for SEBFs: group for number of storeys.

SEBFs—L_b

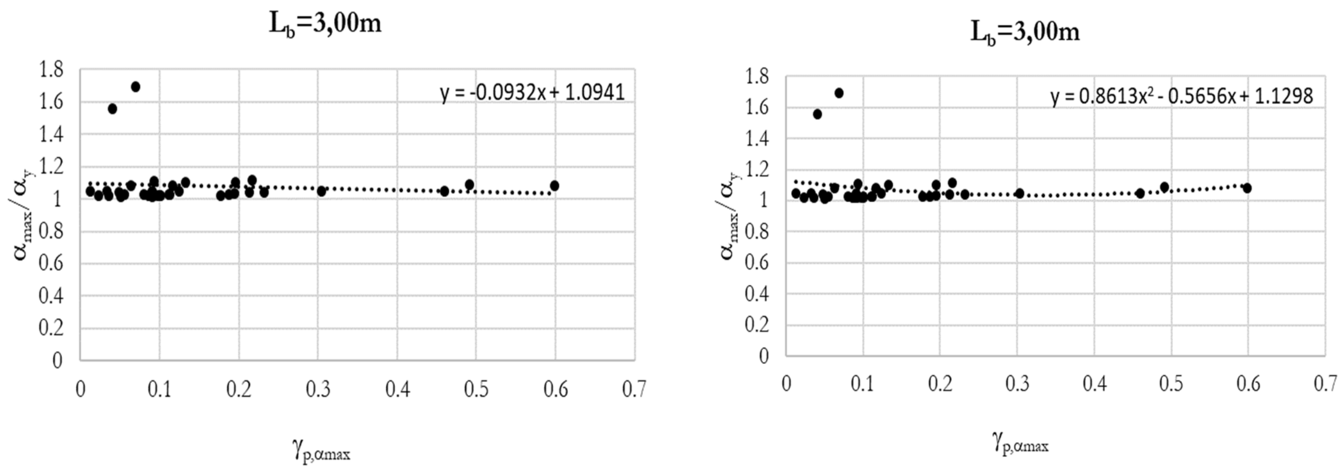

Figure 14. *Cont.*

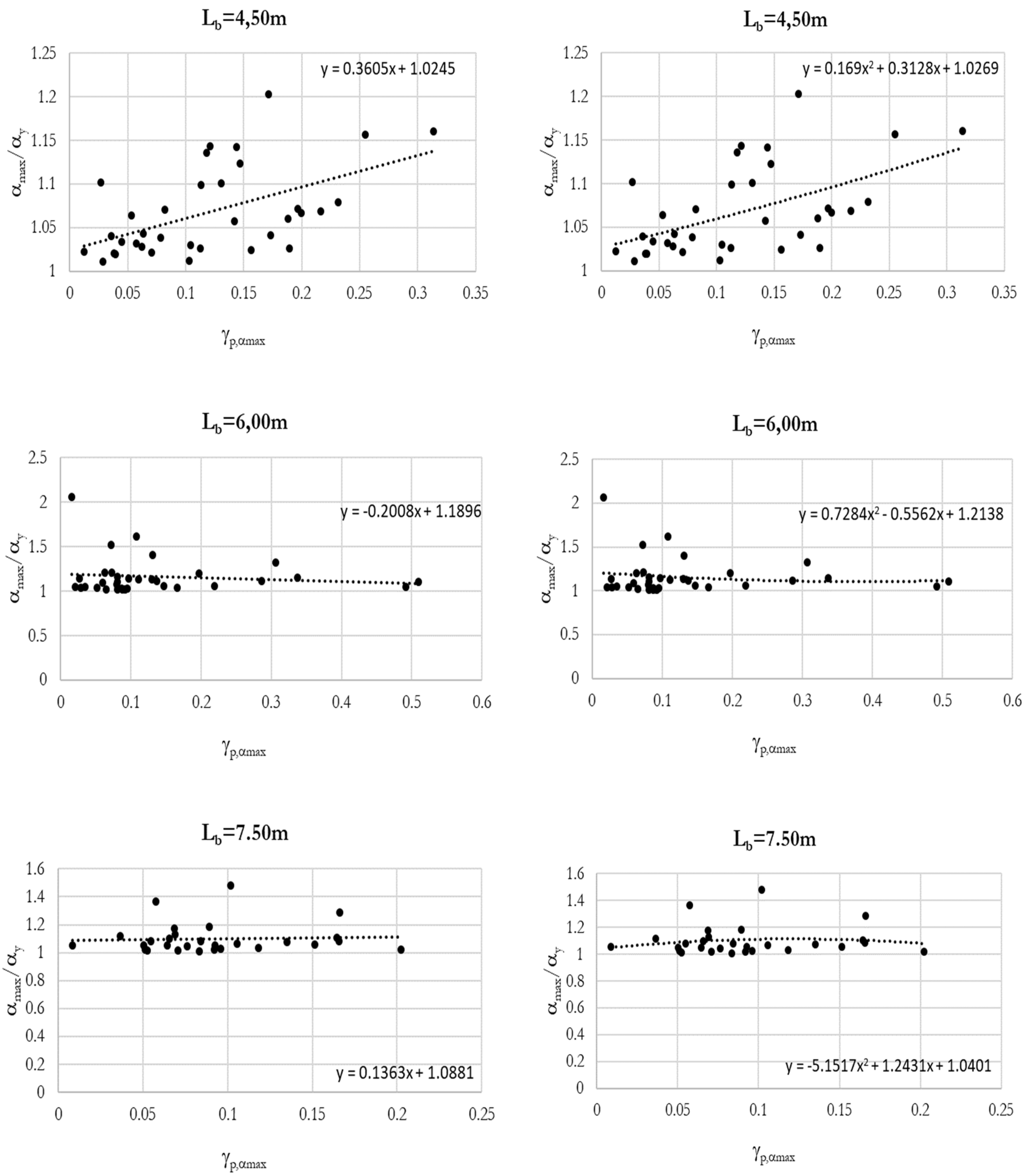

Figure 14. $\frac{\alpha_{max}}{\alpha_y} - \gamma_{p.\alpha_{max}}$ diagram for SEBFs: group for bay span.

For GEBFs in Figures 15–17, the results for the groups n_b (number of bays), n_s (number of storeys), and L_b (bay span) are reported.

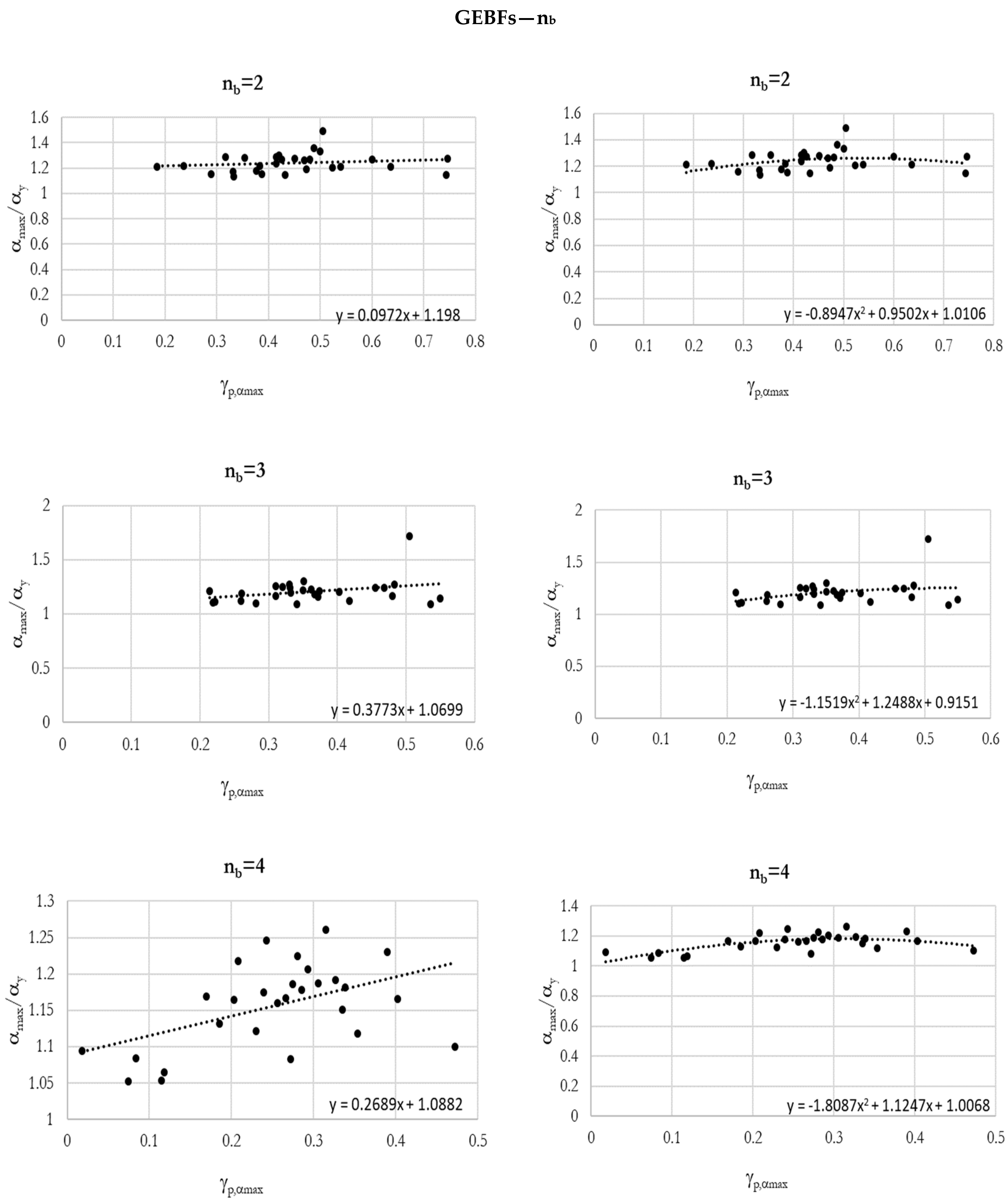

Figure 15. *Cont*.

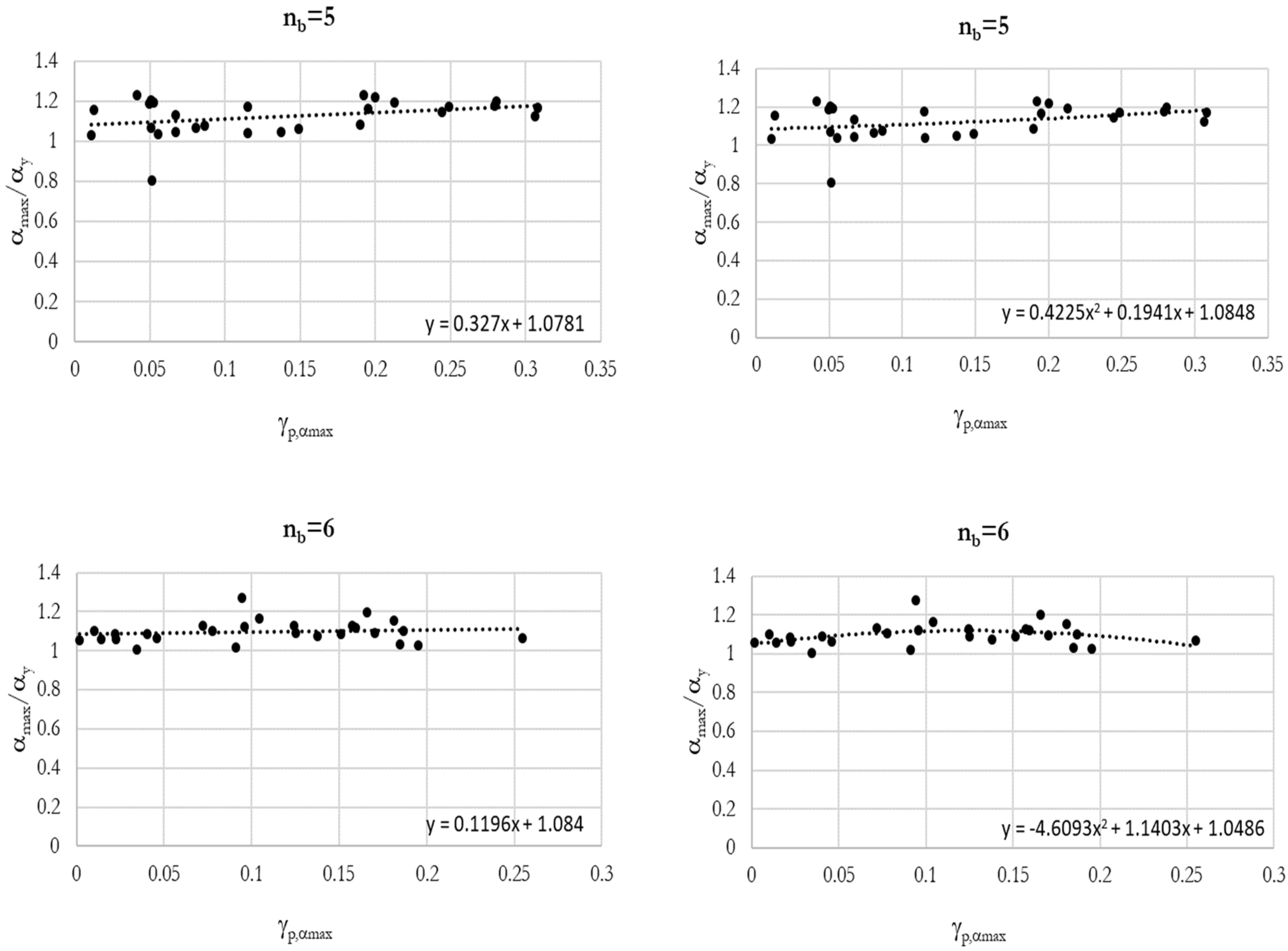

Figure 15. $\frac{\alpha_{max}}{\alpha_y} - \gamma_{p.\alpha_{max}}$ diagram for GEBFs: group for number of bays.

GEBFs—n_s

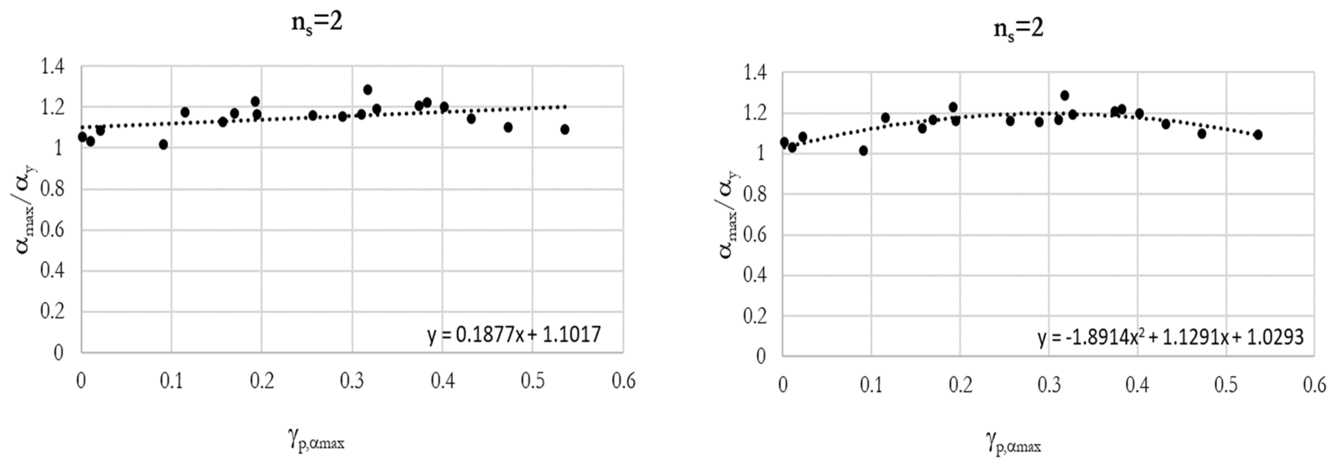

Figure 16. *Cont.*

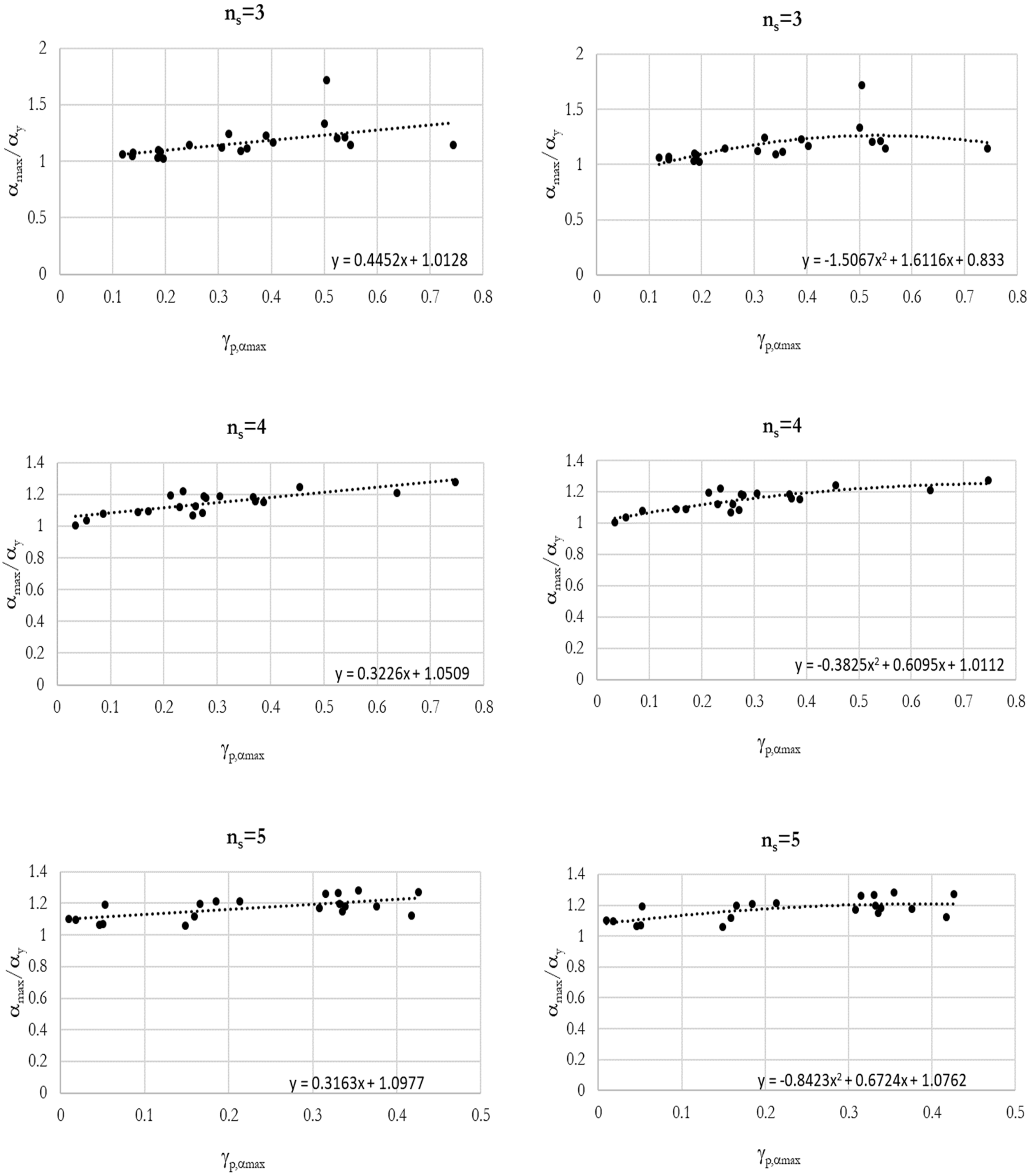

Figure 16. *Cont*.

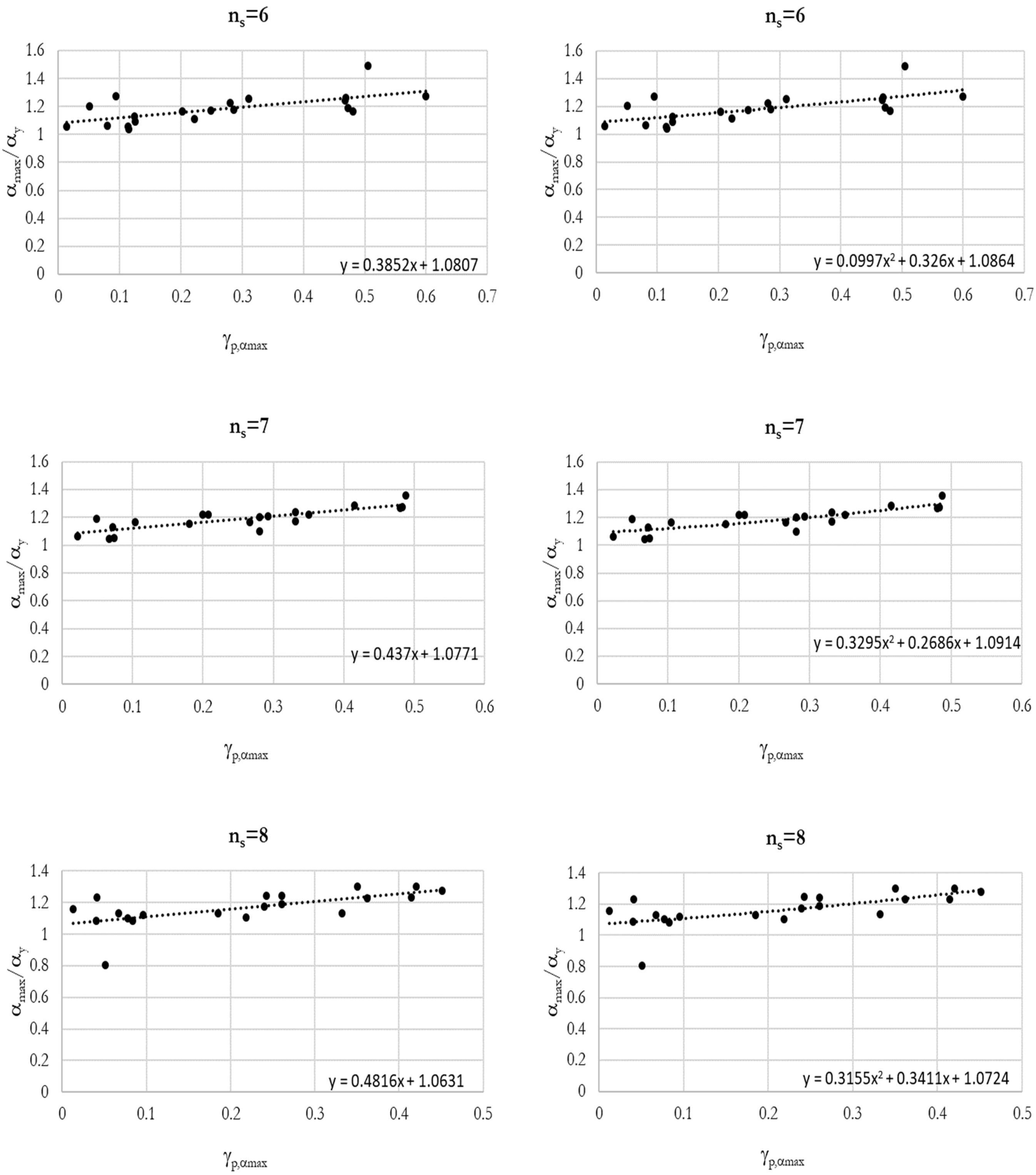

Figure 16. $\frac{\alpha_{max}}{\alpha_y} - \gamma_{p.\alpha_{max}}$ diagram for GEBFs: group for number of storeys.

GEBFs—Lb

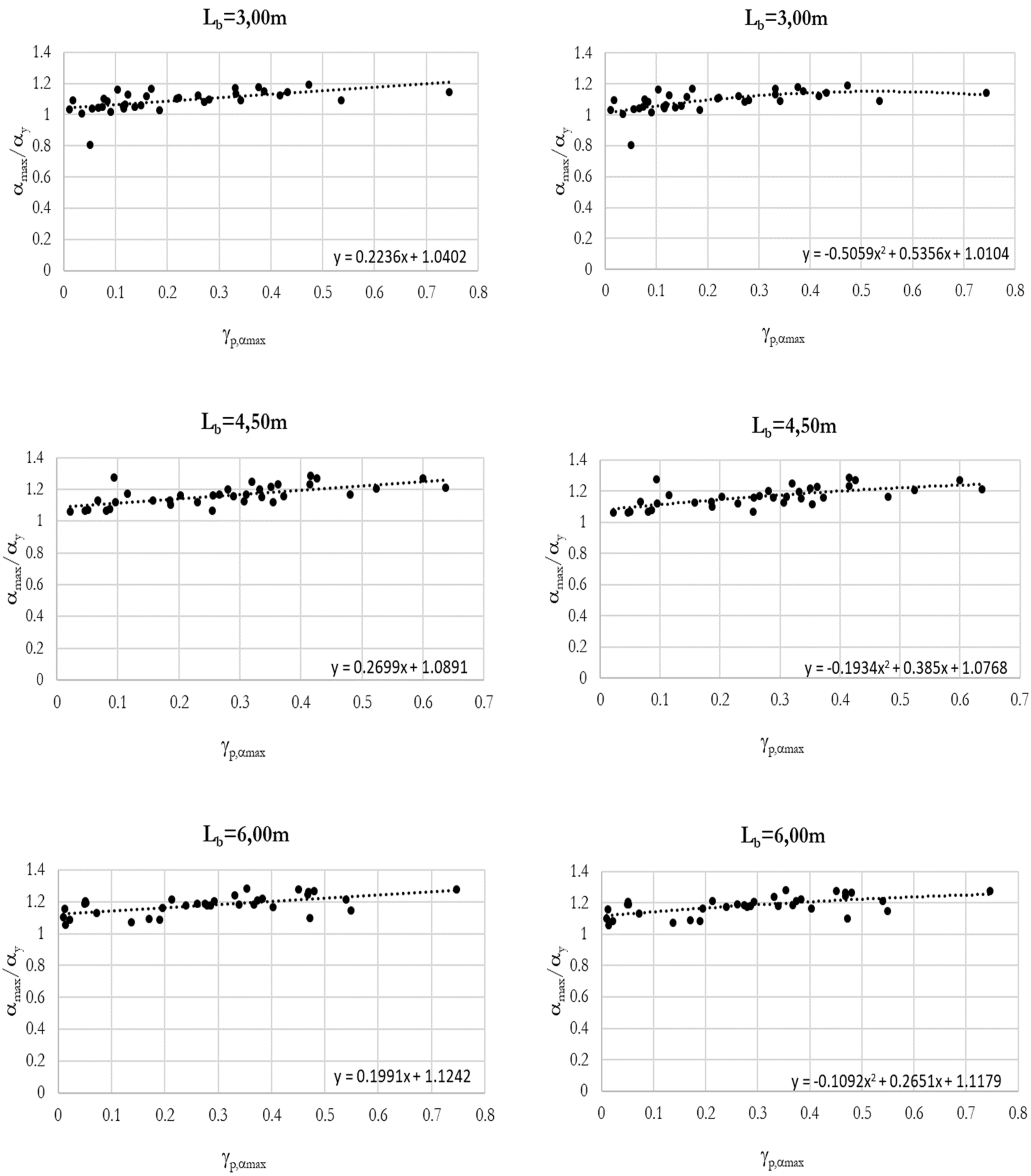

Figure 17. *Cont*.

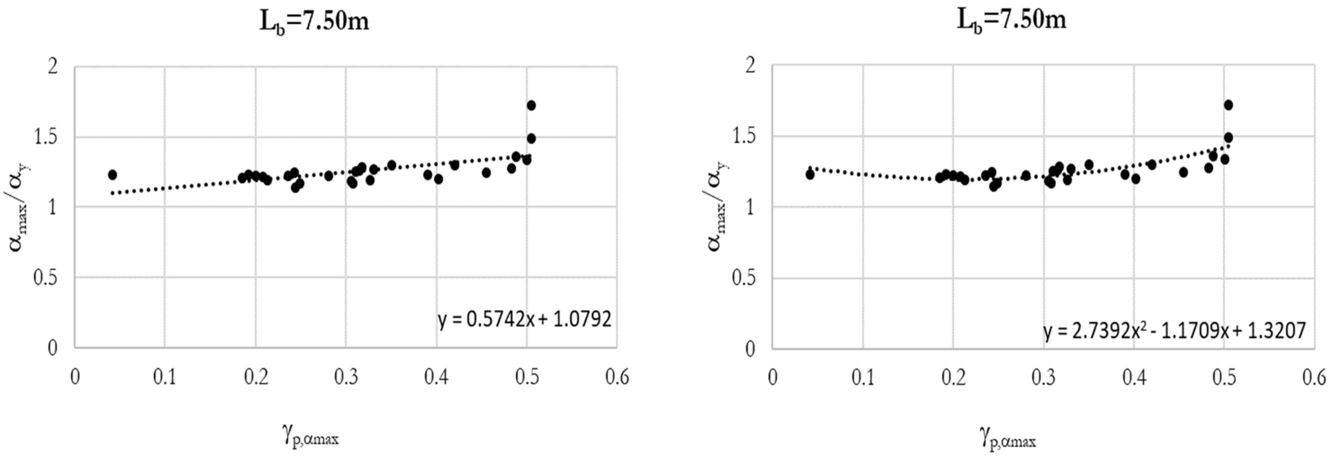

Figure 17. $\frac{\alpha_{max}}{\alpha_y} - \gamma_{p.\alpha_{max}}$ diagram for GEBFs: group for bay span.

Analyzing Figures 12–17, it is evident that there is a direct correspondence between the plastic redistribution capacity α_{max}/α_y and the demand in terms of plastic rotations. $\gamma_{p.\alpha_{max}}$. This direct proportionality is most evident for GEBFs for both linear and parabolic prediction. For SEBFs, in some cases, higher values of α_{max}/α_y do not correspond to higher values of $\gamma_{p.\alpha_{max}}$. This is the case of buildings characterized by $n_b = 2$ and n_s equal to 2, 4, for which the trend is decreasing, constant, or increasing–decreasing. In general, there are some groupings that show a non-direct proportionality between plastic redistribution capacity and demand in terms of plastic rotations at the end of the links and these groupings can be identified mainly for SEBFs type structures. Consequently, from the analysis of Figures 12–17, it is possible to define the range of applicability of the proposed formulation (Equation (37)).

7. Conclusions

The work herein presented allowed us to define a simplified method for the evaluation of demand in terms of plastic rotation of the ends of short links for steel EBF (Eccentrically Braced Frames) type structures. The demand refers to the performance levels provided for by the codes in force and to the achievement of the maximum bearing capacity.

The proposed solution is a fully analytical methodology that exploits elastic analysis and rigid-plastic analysis extended to the second-order effects. The calibration of this relationship was carried out on 420 EBFs equipped with short links designed according to three different approaches. The methodology remains valid if the design assumptions considered in the calibration process are respected.

The results achieved show a good level of precision, as evidenced by the results of the regression analysis, characterized by trend line and determination coefficient R^2 close to the unit.

The 420 frames designed are also used to analyze the behavior in the plastic phase of EBF type structures equipped with short links.

From this analysis it was possible to deduce that SEBFs equipped with short links exceed the rotational limit imposed for Collapse prevention (CP) by 30%, the limit imposed for Life Safety (LS) by 40%, and the limit imposed for the elastic threshold by 70%, while GEBFs equipped with short links exceed the rotational limit imposed for Collapse prevention (CP) by 65%, the limit imposed for Life Safety (LS) by 70%, and the limit imposed for the elastic threshold by 75%.

The study is also accompanied by an extensive analysis on the influence of plastic redistribution capacity on demand in terms of plastic rotations at the ends of the links, corresponding to the achievement of the maximum bearing capacity.

In particular, the GEBFs showed a direct correspondence between plastic redistribution capacity and demand in terms of plastic rotations, confirming the need for higher ductility resources to ensure the development of a global collapse mechanism. Contrastingly, SEBFs have been shown to require fewer ductile resources to achieve maximum bearing capacity but develop partial collapse mechanisms.

The obtained relation can be exploited both as an assessment and as a design tool.

In the first case, this is done by comparing the demand in terms of plastic rotation with the link capacity. In the second case, this is done by predicting the required ultimate plastic rotation as a function of the plastic redistribution capacity of the structure.

The work carried out is aimed at two objectives. The first is to extend this methodology to other design philosophies, thus expanding the field of application of the method. The second is the possibility of making the model more flexible and able to consider additional variables that influence the structural behavior of EBFs.

Author Contributions: R.M.: Conceptualization, Methodology, Writing—Review & Editing, Supervision; E.N.: Software, Validation, Resources, Data Curation, Writing—Review & Editing, Supervision; V.P.: Conceptualization, Methodology, Writing—Review & Editing, Supervision; P.T.: Software, Validation, Writing—Original Draft, Investigation, Formal analysis. All authors have read and agreed to the published version of the manuscript.

Funding: The research leading to the results presented in this paper has received funding from the Italian Department of Civil Protection (DPC-Reluis).

Institutional Review Board Statement: Not applicable.

Informed Consent Statement: Not applicable.

Acknowledgments: The support of DPC-RELUIS 2019–2021 is gratefully acknowledged.

Conflicts of Interest: The authors declare no conflict of interest. The funders had no role in the design of the study; in the collection, analyses, or interpretation of data; in the writing of the manuscript, or in the decision to publish the results.

References

1. Jung, H.-C.; Jung, J.-S.; Lee, K.S. Seismic performance evaluation of internal steel frame connection method for seismic strengthening by cycling load test and nonlinear analysis. *J. Korea Concr. Inst.* **2019**, *31*, 79–88. [CrossRef]
2. Montuori, R.; Nastri, E.; Piluso, V. Problems of modeling for the analysis of the seismic vulnerability of existing buildings. *Ing. Sismica* **2019**, *36*, 53–85.
3. Gupta, A.; Krawinkler, H. Feasibility of Push-Over Analyses for Estimation of Strength Demand. In *Stessa 2003, Behaviour of Steel Structures in Seismic Areas, Proceedings of the 4th Conference on Behaviour of Steel Structures in Seismic Areas, Naples, Italy, 9–12 June 2003*; A.A. Balkema: Lisse, The Netherlands, 2003.
4. Montuori, R.; Nastri, E.; Piluso, V.; Pisapia, A. Probabilistic approach for local hierarchy criteria of EB-frames [Approccio probabilistico per criterio di gerarchia locale di controventi eccentrici (EBFs)]. *Ing. Sismica* **2020**, *37*, 45–64.
5. Montuori, R.; Nastri, E.; Piluso, V. Preliminary analysis on the influence of the link configuration on seismic performances of MRF-EBF dual systems designed by TPMC. *Ing. Sismica* **2016**, *33*, 52–64.
6. Montuori, R.; Nastri, E.; Piluso, V. Seismic response of EB-frames with inverted Y-scheme: TPMC versus eurocode provisions. *Earthq. Struct.* **2015**, *8*, 1191–1214. [CrossRef]
7. *NTC 2018 Italian Code*. Chapter 7 Design for Seismic Actions.
8. Fajfar, P. A Nonlinear Analysis Method for Performance-Based Seismic Design. *Earthq. Spectra* **2000**, *16*, 573–592. [CrossRef]
9. Manganiello, L.; Montuori, R.; Nastri, E.; Piluso, V. The influence of the axial restraint on the overstrength of short links. *J. Constr. Steel Res.* **2021**, *184*, 106758. [CrossRef]
10. Okazaki, T.; Arce, G.; Ryu, H.C.; Engelhardt, M.D. Recent Research on Link Performance in Steel Eccentrically Braced Frames. In Proceedings of the 13th World Conference on Earthquake Engineering, Vancouver, BC, Canada, 1–6 August 2004; Paper Number 302.
11. Okazaki, T.; Arce, G.; Ryu, H.C.; Engelhardt, M.D. Experimental Study of Local Buckling, Overstrength, and Fracture of Links in Eccentrically Braced Frames. *J. Struct. Eng.* **2005**, *131*, 1526–1535. [CrossRef]
12. Okazaki, T.; Engelhardt, M.D.; Drolias, A.; Schell, E.; Hong, J.K.; Uang, C.M. Experimental Investigation of Link-to-Column Connections in Eccentrically Braced Frames. *J. Constr. Steel Res.* **2009**, *65*, 1401–1412. [CrossRef]
13. Okazaki, T.; Engelhardt, M.D. Cyclic loading behavior of EBF links constructed of ASTN A992 steel. *J. Constr. Steel Res.* **2007**, *63*, 751–765. [CrossRef]
14. Bozkurt, M.B.; Topkaya, C. Replaceable Links with Direct Brace Attachments for Eccentrically Braced Frames. *J. Int. Assoc. Earthq. Eng.* **2017**, *46*, 2121–2139. [CrossRef]

15. Bozkurt, M.B.; Topkaya, C. Replaceable Links with Gussed Brace Joints for Eccentrically Braced Frames. *Soil Dyn. Earthq. Eng.* **2018**, *115*, 305–318. [CrossRef]
16. Bozkurt, M.B.; Azad, S.K.; Topkaya, C. Low-Cycle Fatigue Testing of Shear Links and Calibration of a Damage Law. *J. Struct. Eng.* **2018**, *144*, 04018189. [CrossRef]
17. Maalek, S.; Adibrad, M.H.; Moslehi, Y. An Expirimental Investigation of the Behaviour of EBFs. *Struct. Build.* **2012**, *165*, 179–198. [CrossRef]
18. Yin, Z.; Feng, D.; Yang, W. Damage analysis of Replaceable Links in Eccentrically Braced Frames (EBF) Subject to Cyclic Excitation. *Appl. Sci.* **2018**, *8*, 1–20.
19. Ji, X.; Wang, Y.; Ma, Q.; Okazaki, T. Cyclic Behavior of Very Short Steel Shear Links. *J. Struct. Eng.* **2016**, *142*, 04015114. [CrossRef]
20. Mansour, N.; Christopoulos, C.; Tremblay, R. Experimental Validation of Replaceable Shear Links for Eccentrically Braced Steel Frames. *J. Struct. Eng.* **2011**, *137*, 1141–1152. [CrossRef]
21. Lian, M.; Su, M. Experimental Study and Simplified Analysis of EBF Fabricated with High Strength Steel. *J. Constr. Steel Res.* **2017**, *139*, 6–17. [CrossRef]
22. Badalassi, M.; Braconi, A.; Caprili, S.; Salvatore, W. Influence of steel mechanical properties on EBF seismic behaviour. *Bull. Earthq. Eng.* **2013**, *11*, 2249–2285. [CrossRef]
23. *EN 1998-1*; Eurocode 8: Design of Structures for Earthquake Resistance—Part 1: General Rules, Seismic Actions and Rules for Buildings. CEN: Brussels, Belgium, 2004.
24. *UNI EN 1993-1-1*; Eurocode 3: Design of steel structures Part 1-1: General rules and rules for buildings. CEN: Brussels, Belgium, 2005.
25. *EN 1998-3*; Eurocode 8: Design of Structures for Earthquake Resistance—Part 3: Assessment and retrofitting of buildings. CEN: Brussels, Belgium, 2004.
26. Montuori, R.; Nastri, E.; Piluso, V. Rigid-plastic analysis and moment-shear interaction for hierarchy criteria of inverted y EB-Frames. *J. Constr. Steel Res.* **2014**, *95*, 71–80. [CrossRef]
27. Montuori, R.; Nastri, E.; Piluso, V. Theory of plastic mechanism control for eccentrically braced frames with inverted y-scheme. *J. Constr. Steel Res.* **2014**, *92*, 122–135. [CrossRef]
28. Mastrandrea, L.; Nastri, E.; Piluso, V. Validation of a design procedure for failure mode control of EB-Frames: Push-over and IDA analyses. *Open Constr. Build. Technol. J.* **2013**, *7*, 193–207. [CrossRef]
29. Naeim, F. Earthquake Engineering—From Engineering Seismology to Performance-Based Engineering. *Earthq. Spectra* **2005**, *21*, 609–611. [CrossRef]
30. Longo, A.; Montuori, R.; Piluso, V. Moment frames–concentrically braced frames dual systems: Analysis of different design criteria. *Struct. Infrastruct. Eng.* **2016**, *12*, 122–141. [CrossRef]
31. Piluso, V.; Montuori, R.; Nastri, E.; Paciello, A. Seismic response of MRF-CBF dual systems equipped with low damage friction connections. *J. Constr. Steel Res.* **2019**, *154*, 263–277. [CrossRef]
32. Montuori, R.; Nastri, E.; Piluso, V.; Todisco, P. A simplified performance-based approach for the evaluation of seismic performances of steel frames. *Eng. Struct.* **2020**, *224*, 111222. [CrossRef]
33. Montuori, R.; Nastri, E.; Piluso, V.; Todisco, P. Evaluation of the seismic capacity of existing moment resisting frames by a simplified approach: Examples and numerical application. *Appl. Sci.* **2021**, *11*, 2594. [CrossRef]
34. Nastri, E.; Vergato, M.; Latour, M. Performance evaluation of a seismic retrofitted R.C. precast industrial building. *Earthq. Struct.* **2017**, *12*, 13–21. [CrossRef]
35. Bruneau, M.; Uang, C.M.; Sabelli, R.S.E. *Ductile Design of Steel Structures*; McGraw-Hill: New York, NY, USA, 2011.
36. Montuori, R.; Nastri, E.; Piluso, V. Advances in theory of plastic mechanism control: Closed form solution for MR-Frames. *Earthq. Eng. Struct. Dyn.* **2015**, *44*, 1035–1054. [CrossRef]
37. Piluso, V.; Pisapia, A.; Castaldo, P.; Nastri, E. Probabilistic Theory of Plastic Mechanism Control for Steel Moment Resisting Frames. *Struct. Saf.* **2019**, *76*, 95–107. [CrossRef]
38. Computer and Structure Inc. *SAP2000: Integrated Finite Element Analysis and Design of Structures. Analysis Reference*; Computer and Structure Inc.; University of California: Berkeley, CA, USA, 2007.
39. Mazzolani, F.M.; Piluso, V. Plastic Design of Seismic Resistant Steel Frames. *Earthq. Eng. Struct. Dyn.* **1997**, *26*, 167–191. [CrossRef]
40. Mazzolani, F.M.; Piluso, V. *Theory and Design of Seismic Resistant Steel Frames*; E&FN Spon: London, UK, 1996.
41. Yun, S.Y.; Hamburger, R.O.; Cornell, C.A.; Foutch, D.A. Seismic performance evaluation for steel moment frames. *J. Struct. Eng.* **2002**, *128*, 534–545. [CrossRef]